UNIVERSITY OF HELSINKI REPORT SERIES IN PHYSICS

HU-P-D137

Irradiation-mediated tailoring of carbon nanotubes

Jani Kotakoski

Accelerator Laboratory
Department of Physical Sciences
Faculty of Science
University of Helsinki
Helsinki, Finland

ACADEMIC DISSERTATION

To be presented, with the permission of the Faculty of Science of the University of Helsinki, for public criticism in the lecture room E204 of the Department of Physical Sciences (Physicum), on March the 31st, 2007, at 12 o'clock p.m.

HELSINKI 2007

ISBN 978-952-10-3239-4 (printed version)
ISSN 0356-0961
Helsinki 2007
Helsinki University Printing House (Yliopistopaino)

ISBN 978-952-10-3240-0 (PDF version)
http://ethesis.helsinki.fi/
Helsinki 2007
Electronic Publications @ University of Helsinki (Helsingin yliopiston verkkojulkaisut)

Jani Kotakoski: **Irradiation-mediated tailoring of carbon nanotubes**, University of Helsinki, 2007, 50 p.+appendices, University of Helsinki Report Series in Physics, HU-P-D137, ISSN 0356-0961, ISBN 978-952-10-3239-4 (printed version), ISBN 978-952-10-3240-0 (PDF version)

Classification (INSPEC): A6185, A6148, A6180J
Keywords (INSPEC): carbon nanotubes, radiation effects, simulation

ABSTRACT

The ever-increasing demand for faster computers in various areas, ranging from entertaining electronics to computational science, is pushing the semiconductor industry towards its limits on decreasing the sizes of electronic devices based on conventional materials. According to the famous law by Gordon E. Moore, a co-founder of the world's largest semiconductor company Intel, the transistor sizes should decrease to the atomic level during the next few decades to maintain the present rate of increase in the computational power. As leakage currents become a problem for traditional silicon-based devices already at sizes in the nanometer scale, an approach other than further miniaturization is needed to accomplish the needs of the future electronics.

A relatively recently proposed possibility for further progress in electronics is to replace silicon with carbon, another element from the same group in the periodic table. Carbon is an especially interesting material for nanometer-sized devices because it forms naturally different nanostructures. Furthermore, some of these structures have unique properties. The most widely suggested allotrope of carbon to be used for electronics is a tubular molecule having an atomic structure resembling that of graphite. These *carbon nanotubes* are popular both among scientists and in industry because of a wide list of exciting properties. For example, carbon nanotubes are electronically unique and have uncommonly high strength versus mass ratio, which have resulted in a multitude of proposed applications in several fields. In fact, due to some remaining difficulties regarding large-scale production of nanotube-based electronic devices, fields other than electronics have been faster to develop profitable nanotube applications.

In this thesis, the possibility of using low-energy ion irradiation to ease the route towards nanotube applications is studied through atomistic simulations on different levels of theory. Specifically, molecular dynamic simulations with analytical interaction models are used to follow the irradiation process of nanotubes to introduce different impurity atoms into these structures, in order to gain control on their electronic character. Ion irradiation is shown to be a very efficient method to replace carbon atoms with boron or nitrogen impurities in single-walled nanotubes. Furthermore, potassium irradiation of multi-walled and fullerene-filled nanotubes is demonstrated to result in small potassium clusters in the hollow parts of these structures. Molecular dynamic simulations are further used to

give an example on using irradiation to improve contacts between a nanotube and a silicon substrate. Methods based on the density-functional theory are used to gain insight on the defect structures inevitably created during the irradiation. Finally, a new simulation code utilizing the kinetic Monte Carlo method is introduced to follow the time evolution of irradiation-induced defects on carbon nanotubes on macroscopic time scales.

Overall, the molecular dynamic simulations presented in this thesis show that ion irradiation is a promising method for tailoring the nanotube properties in a controlled manner. The calculations made with density-functional-theory–based methods indicate that it is energetically favorable for even relatively large defects to transform to keep the atomic configuration as close to the pristine nanotube as possible. The kinetic Monte Carlo studies reveal that elevated temperatures during the processing enhance the self-healing of nanotubes significantly, ensuring low defect concentrations after the treatment with energetic ions. Thereby, nanotubes can retain their desired properties also after the irradiation. Throughout the thesis, atomistic simulations combining different levels of theory are demonstrated to be an important tool for determining the optimal conditions for irradiation experiments, because the atomic-scale processes at short time scales are extremely difficult to study by any other means.

Contents

1 INTRODUCTION

In order to meet the ever-increasing demand for more computer power, scientists have been searching for alternatives to replace silicon as the building material for electronics. After the research on properties of carbon nanotubes (CNTs) started in the early 1990s [1], they have been one of the most promising materials for smaller next-generation devices [2]. Other applications for these molecules are based on their unique thermal and optical properties as well as on the combination of their lightness and mechanical strength.

Nanotubes consist of honeycomb-like layers of carbon atoms (similar to graphite sheets) rolled up to form a seamless tube. The empty space inside the structure makes nanotubes very light, yet the strong graphitic carbon-carbon bonds give these cylinders strength exceeding that of metal wires of similar size. The typical diameters of nanotubes are some nanometers, and their lengths are in the micrometer regime. The length depends mostly on the geometry of the system used for their growth, and the upper limit is set only by imagination (current world record is 4 cm for a single-walled nanotube [3]). As the atomic structure of nanotubes is well defined, and repeated periodically over the structure, they in this sense resemble crystalline solids, while their size is in the range usually related to large molecules. Curiously, the orientation of the atoms in each nanotube defines their electric nature – a unique property of this material. Depending on this orientation, *i.e.* the *chirality* of each tube, described by only two integers, the *chiral indices*, CNTs are either metallic or semiconducting [4].

Although CNTs have very exciting properties, some problems remain to be solved before their full potential can be utilized in applications for electronics. One barrier to overcome is due to the inertness of nanotube walls, which makes it difficult to functionalize them or to contact them properly. This is clearly demonstrated by the fact that although individual high-purity single-walled carbon nanotubes (SWNTs) have excellent mechanical properties, the values measured for samples consisting of several tubes are not in the same range [5]. As for electronics, in addition to the problems with contacting the tubes, another severe problem is that the as-grown nanotube samples are always mixtures of nanotubes with different chiralities, and thus different electrical properties. Hence, a time consuming process of separating and testing the tubes has to be performed before they can be used for any specific application. This obviously prevents large-scale manufacturing of nanotube devices.

The studies presented in this thesis demonstrate possible ways to overcome, at least partially, some of these problems by using ion irradiation. Despite the recent advances in experimental techniques [6; 7], the atomic-scale analysis of irradiation-induced phenomena in nanostructures is extremely difficult, so that we have utilized atomistic simulations with different levels of theory for this purpose. The molecular dynamics (MD) method with analytical potentials is suitable for understanding interacting

energetic particles, such as in irradiation events, when the time scale is some nanoseconds. Assuming that the analytical model used in the simulations describes properly the properties of the system, MD can be used to obtain detailed information on these processes at the atomic level. However, to ensure that the structures given by this method are physically correct, they have to be confirmed with higher-accuracy calculations using methods such as density-functional theory (DFT) or density-functional-theory–based tight-binding (DFTB). For applications, also the evolution of the irradiated systems has to be known on time scales longer than those reachable with MD. For this purpose, we have developed a new simulation code based on the kinetic Monte Carlo (KMC) method. While involving even more approximations than MD, it can be used to simulate structures with macroscopic sizes at time scales of experimental relevance.

2 PURPOSE AND STRUCTURE OF THIS STUDY

The purpose of this thesis is to understand how irradiation with charged particles, specifically ions, can be used to overcome different problems currently faced within CNT research on the way towards applications, and to increase the understanding of the response of nanotubes to irradiation via diffusion and coalescence of irradiation-induced defects. As computational methods are used to achieve these goals, the results are compared with experiments whenever experimental data exists to ensure the predictive power of our studies.

This thesis consists of this summary and five articles (referred to by bold face Roman numerals) which are either published or accepted for publication in international peer-reviewed journals. In this section, the articles are summarized and the contribution of the author to these publications is explained. In section 3, the basic properties and applications of CNTs are presented as a necessary background information. Section 4 shortly describes the methods used in the studies of this thesis. In section 5, the results from atomistic simulations of irradiation of CNTs are presented. Finally, the thesis is concluded in section 6.

2.1 Summaries of the original publications

In publication **I**, doping of a SWNT using low-energy boron and nitrogen irradiation is studied with MD simulations. The resulting defect structures including the dopant atoms are analyzed and their stability is ensured with DFT calculations. Publication **II** continues on using MD simulations on studying ion irradiation-induced doping. This time, however, the dopant is potassium and the irradiated nanotubes have many walls. Binding a SWNT to silicon surface using irradiation with silicon,

carbon and neon ions is studied with MD in publication **III**. In publication **IV**, the DFTB method is utilized for finding the minimum-energy configurations for multivacancy structures on a SWNT. Calculations using an empirical interaction model and the DFT method are also used to investigate the interaction between single vacancies. Publication **V** introduces a new KMC–based simulation code for modeling diffusion and coalescence of irradiation-induced defects on nanotube walls. As a test of the code, it is applied to studying the irradiation response of nanotubes under a transmission electron microscope (TEM) at various temperatures.

Publication I: B and N implantation onto carbon nanotubes: insight from atomistic simulations, J. Kotakoski, A. V. Krasheninnikov, Y. Ma, A. S. Foster, K. Nordlund and R. M. Nieminen, *Physical Review B* **71**, 205408 (2005).

> This publication presents MD simulations on low-energy irradiation of SWNTs with boron and nitrogen ions. With an optimal energy of about 50 eV, the dopants are shown to most likely obtain the substitutional position in the nanotube atomic network by perfectly replacing a carbon atom. The maximum probability of the substitution is found to be nearly 30 % for boron and about 40 % for nitrogen. In the second and third most probable structures after the irradiation, the replaced carbon atom remains also attached to the defect structure. Stability of the most prolific structures is discussed in terms of density-functional theory calculations. The bonding energy for the dopants, especially for boron, is found to be low enough to allow on-surface diffusion, if the dopant is not in the perfect substitutional lattice site, possibly further increasing the substitution probability.

Publication II: A molecular dynamics study of the clustering of implanted potassium in multiwalled carbon nanotubes, J. Kotakoski, A. V. Krasheninnikov and K. Nordlund, *Nuclear Instruments and Methods in Physics Research B* **240**, 810 (2005).

> Potassium irradiation of multi-walled carbon nanotubes is studied in this publication with MD simulations. The optimum energy needed for a potassium atom to penetrate a certain number of graphitic layers is first studied in order to estimate the energy range suitable for doping of nanotubes with 1–5 coaxial walls. With reasonable energies, the irradiation is shown to result in small potassium clusters in the hollow parts of the tubes. Due to the differences between potassium and boron/nitrogen, both in size and in chemistry, it is highly unlikely for a potassium atom to be incorporated to the nanotube atomic network. For nanotubes with 1–3 walls the optimum irradiation energy is found to be around 100 eV. Ions with energies lower than this are not able to penetrate the nanotube walls while higher energies are more likely to destroy the structure. The optimum energy is expected to increase with increasing system size.

Publication III: Binding a carbon nanotube to the Si (100) surface using ion irradiation - an atomistic simulation study, J. Kotakoski and K. Nordlund, *New Journal of Physics* **8**, 115 (2006).

The most obvious route towards CNT–based electronic devices is to first integrate nanotubes and the existing silicon technology. In this publication, MD simulations are used to study whether ion irradiation can be used to enhance the contacts between CNTs and silicon substrates. Irradiation is performed with carbon, neon and silicon ions. The nanotube is deposited over a trench created to the silicon substrate, after which the structure is uniformly irradiated. This geometry allows utilizing the differences between the irradiation-induced damage production on suspended and on-substrate nanotubes for preventing unwanted destruction of certain parts of the nanotube. Ion irradiation is shown to result in new covalent bonds at the contact areas, typically $0.5 - 0.9 \times (10^{14}$ ions/cm$^2)^{-1}$, while increasing the binding energy at the same time by $100 - 400\%$.

Publication IV: Energetics, structure and long-range interaction of vacancy-type defects in carbon nanotubes: Atomistic simulations, J. Kotakoski, A. V. Krasheninnikov and K. Nordlund, *Physical Review B* **74**, 245420 (2006).

Atomic vacancies are, along with interstitial atoms, the most prolific defects caused by irradiation of CNTs. In this publication, the properties of multivacancies with up to six missing atoms are studied with density-functional-theory–based tight-binding method. Large "holes" are found to be very unlikely to form via coalescing of single vacancies. Instead, chain-like structures parallel to the nanotube axis are preferred, and defects with six or more missing atoms are found to most likely split into smaller defects separated by perfect hexagons. Also a preference of even-numbered vacancies is evident over the odd-numbered ones due to more effective dangling bond saturation. Calculations using an empirical interaction model and the DFT method are also used to study the vacancy-vacancy interaction, which is surprisingly found to consist both of a mechanical strain effect and of an electrical effect, and to be in the milli-eV range.

Publication V: Kinetic Monte Carlo simulations of the response of carbon nanotubes to electron irradiation, J. Kotakoski, A. V. Krasheninnikov and K. Nordlund, *Journal of Computational and Theoretical Nanoscience, accepted for publication.*

In this publication, a new KMC–based simulation code for defect diffusion and coalescence on CNTs is introduced. Input parameters for the method are obtained from DFT–based calculations. The code can be used to model the diffusion process on a SWNT with any chirality and

diameter, and the time evolution of systems with lengths up to micrometers can easily be followed for several seconds. As a test, the method is applied on studying the irradiation response of SWNTs at different temperatures under a transmission electron microscope (TEM). Nearly perfect *in situ* self-healing of nanotubes is observed at temperatures higher than about 300°C, in perfect agreement with the experiments. Also the times needed to cut a nanotube with the TEM are similar to the experimental values, although direct comparison is difficult because of the experimental uncertainties. As a slight surprise, at a temperature range of $130 - 230$°C, the increase in temperature was found to have a negative effect on the self-healing process. However, at higher temperatures, heating always enhances the healing.

2.2 Author's contribution

The author of this thesis carried out all calculations and analysis in publications **II**, **III** and **V**. In publication **I** the author carried out all the MD simulations and in publication **IV** all the empirical interaction model and DFTB calculations, and the analysis related to these simulations in both publications. The new KMC–based simulation code introduced and utilized in publication **V** was developed by the author, and he carried out all the simulations with this code. The author also wrote most of the text in all publications.

3 CARBON NANOTUBES

CNTs are a recently found cylindrical allotrope of carbon. The scientific research on their properties began in 1991 after Sumio Iijima's report on finding of multi-walled carbon nanotubes [1] with a description of their atomic structure. However, also earlier observations had been made [8]. In this section, a short introduction to these fascinating molecules is provided. The section begins with a description of their atomic structure, after which the most important fabrication methods are shortly introduced. In the end, their most outstanding properties and some of their applications are briefly addressed. Main emphasis in this section, and through the whole thesis, is on isolated SWNTs.

3.1 Structure

CNTs are tubular molecules consisting only of elemental carbon. They can be thought as wrapped-up graphite sheets. Except for caps, which are usually found at the ends of the tubes, the atomic structure of a pristine nanotube is similar to a perfect honeycomb network with a carbon atom in each joint,

rolled up to form a seamless tube (figure 1). Similar to a buckminsterfullerene [9], also 5-membered carbon rings are present in the caps enabling the closing of the structure. All carbon atoms have three nearest neighbors and hence all atomic bonds in nanotubes are sp^2-hybridized.

The orientation of the honeycombs in each nanotube with respect to the nanotube axis – the *chirality* – is described with two integers, the *chiral indices* (*n*,*m*). They describe a vector between two crystallographically equivalent atoms of a nanotube in the graphite lattice (see figure 2). The two families of CNTs having symmetric atomic structure, with respect to the tube axis, are given special names; tubes with $m = 0$ are called *zigzag* and those with $n = m$ are called *armchair* nanotubes. All other tubes are simply *chiral*. Examples of these three types of nanotubes are presented in figure 2.

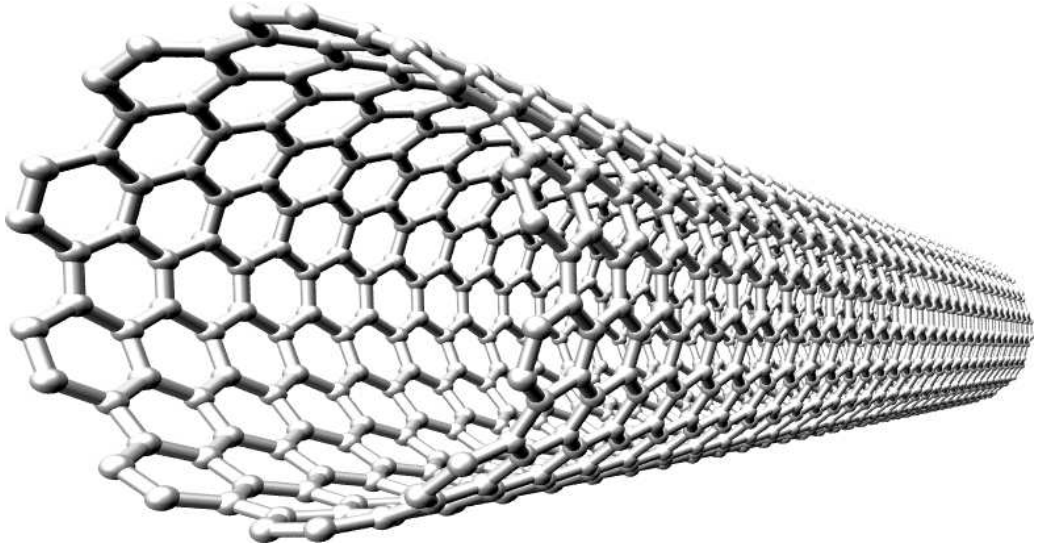

Figure 1: Ball-and-stick presentation of the atomic structure of a (10,10) SWNT.

Nanotubes can have either one or several coaxial walls (*single-walled* and *multi-walled nanotubes*, SWNTs and MWNTs, respectively). The diameter of a nanotube d is defined by the chiral indices as

$$d = b\sqrt{3(n^2 + nm + m^2)}/\pi, \tag{1}$$

where b is the length of the carbon-carbon bond in the structure. The upper limit for the diameter of a SWNT seems to be around seven nanometers, after which the structure becomes energetically unstable, and graphitic layers are favored over nanotubes. However, larger diameters are common for MWNTs, enabled by the support of the inner shells. The minimum diameter $d_{min} \approx 0.35$ nm is near the inter-layer distance in graphite. Typical nanotube lengths are some micrometers and they frequently align in bundles with $\sim$10–100 parallel tubes held together by weak Van der Waals interaction (estimated to have a strength of somewhat less than ~ 1.0 eV/Å [10]).

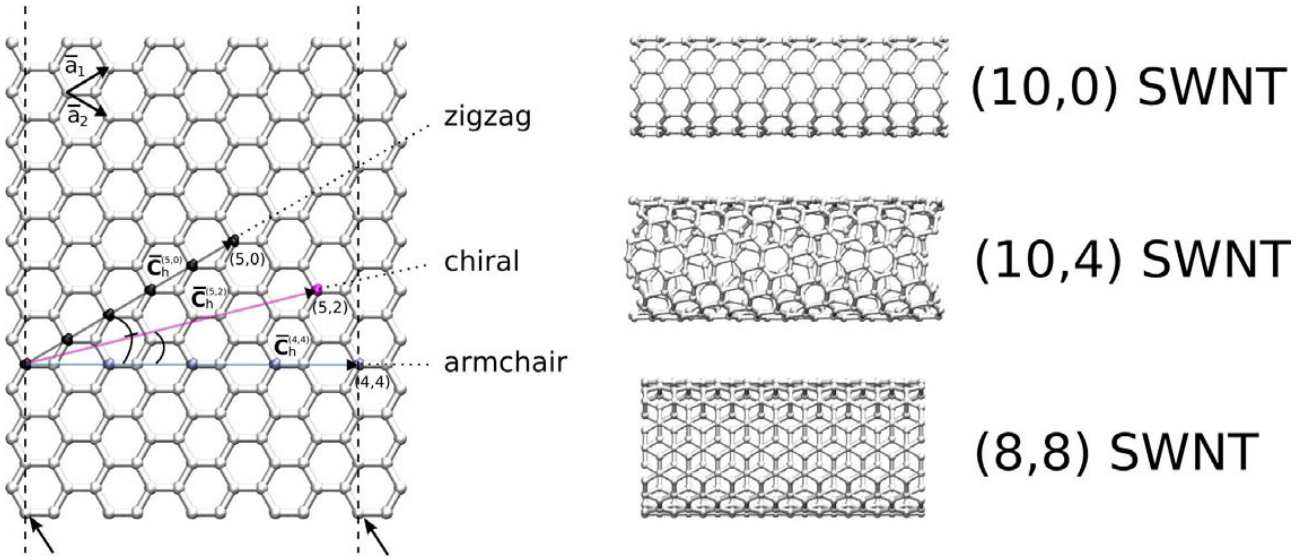

Figure 2: Piece of a single graphite sheet (left) with the graphitic unit vectors $\mathbf{a}_1$ and $\mathbf{a}_2$, and chiral vectors for three different SWNTs marking the atoms forming the circumference of each tube. If cuts are made perpendicular to these vectors at both ends, a nanotube with chiral indices corresponding to the numbers of unit vectors in the chiral vector can be formed. For example, wrapping up the structure between the dashed lines, pointed out by vector ($\mathbf{C}_h{}^{(4,4)} = 4\mathbf{a}_1 + 4\mathbf{a}_2$), by joining the atoms marked with arrows, would lead to a (4,4) SWNT, which is similar to the (8,8) SWNT, presented in the right-hand side, with respect to the orientation of the hexagons, but would have half the diameter of this tube.

3.2 Fabrication

The multi-walled nanotubes reported by Sumio Iijima in 1991 [1] were found in carbon soot made by the arc-discharge method. After two more years the first SWNTs were introduced [11; 12]. During the past decade, several methods have been developed to grow both single-walled and multi-walled nanotubes. The three most widely used methods are arc-discharge, laser ablation and chemical vapor deposition (CVD). Unfortunately none of these methods has been able to grow nanotubes with predefined chiralities. However, very recent advances on the CVD method using short pieces of SWNTs as a seed material for the growth may finally make this possible [13].

Both the arc-discharge and the laser ablation methods are based on condensation of carbon gas, evaporated from a solid source at temperatures near 3500°C. In arc-discharge, carbon is evaporated from a negative electrode due to high temperature caused by the discharge. By controlling the chamber pressure, currents, and the composition of plasma in the chamber, some control can be gained on the properties of the fabricated nanotubes. The mass yield of this method is about 30 % and both single-walled and multi-walled tubes can be produced. The tube lengths are limited to around 50 μm [2].

In laser ablation, intense laser pulses are aimed at the carbon source. An inert gas flow is let to the chamber to carry the carbon material, evaporated by the laser, towards a collector. The nanotubes grow during the cooling of the carried carbon gas. The yield can be as high as 70%, and the produced nanotubes have a uniform diameter distribution, dependent on the chamber temperature. However, the cost of this method is clearly higher than that for either arc-discharge or CVD [2].

Chemical vapor deposition relies on the flow of vaporized hydrocarbon material through a chamber. Nanotubes grow over a heated catalyst material using this vapor as the carbon source. Due to low growing temperatures (around 650°C), the produced tubes often have a high defect concentration. The best catalyst materials are iron, nickel and cobalt nanoparticles. The diameters of the nanotubes can be somewhat controlled with the nanoparticle size [14]. Among the presented growth methods, CVD has the lowest price per mass ratio. In addition, it also allows growing the tubes directly on substrates, and can be used to grow vertically aligned nanotube structures resembling a forest. Given the recent advance in predefining the chirality of the tubes by using small nanotube pieces as a seed material [13], CVD is the most promising candidate for large-scale production of nanotubes for applications requiring strict chirality control.

Because the as-grown nanotube samples frequently contain impurities such as catalyst particles and amorphous carbon, and the tubes are often entangled into a complex network, purification and isolation methods have also been studied widely [15].

3.3 Properties of individual nanotubes

The sp^2-hybridized carbon-carbon bond is one of the strongest known atomic bonds, its strength exceeding even that of the sp^3 bond of diamond. These bonds, combined with the tubular geometry, give nanotubes a strength versus mass ratio among the highest known for any material. For example, the change of stress with strain (the Young's modulus) of MWNTs ($\sim$1.3 TPa), measured with an atomic force microscope by Wong *et al.* [16], is about 56 times higher than that of a steel wire [17]. Due to the nearly one-dimensional structure, nanotubes are very stiff in the axial direction. For larger strains they can buckle, form kinks, or even collapse due to the hollow core. However, these transformations are usually reversible and involve no bond breaking. The irreversible transformations require high deformations [4]. Unfortunately, nanotube bundles and other larger structures do not perform as well as isolated tubes [5], because of the weak Van der Waals interaction between the tubes. Furthermore, the nanotubes in the samples contain always some defects [18] causing deviations from the ideal theoretical values [19].

As there are infinitely many ways to orient the honeycomb lattice to form a seamless cylinder, there are in principle equally many different nanotubes. By its electric character, an isolated graphene sheet is a semiconductor with zero band gap (a semi-metal) having two nonequivalent points in the reciprocal space (k-space) in which the conduction band and the valence band are degenerate. For carbon nanotubes, the periodicity of the lattice around the circumference of the tube discretizes the set of allowed wave numbers for the electron wave functions. Therefore, for some CNTs the allowed numbers include the overlap points making these tubes metallic, whereas for others they do not. Because the chiral indices determine the orientation of the lattice, they also govern the electrical properties of each tube. Based on their electrical properties, carbon nanotubes can be divided into three categories [20]:

(1) metals (for which $n = m$),

(2) very tiny–gap semiconductors (for which $2n + m = 3q$, where q is an integer) and

(3) semiconductors (all other tubes).

For the smallest tubes, the high curvature makes the picture more complicated.

As a graphene sheet can be thought of as a CNT with infinite radius, the band gaps of the semiconducting nanotubes approach zero with increasing diameter [4]. Because of the typical aspect ratio of $1:1000$, the metallic SWNTs present a nearly perfect model system of one-dimensional conductors. They should, according to theory, have a conductance of two times the quantum conductance $2G_0 = 4e^2/h$ [21] (e is the charge of an electron and h is Planck's constant), but due to scatterers, such as impurities and other defects, the measured values are lower. For example, a recent paper [22] relates the resistance of defected nanotubes to the average separation of two divacancies via equation

$$R = R_c + \frac{1}{2G_0} e^{L/L_0}, \tag{2}$$

where R_c is contact resistance, L is the length of the nanotube and L_0 is a localization length related to the divacancy separation. The current carrying capacity of metallic tubes has been shown to exceed 10^9 A/cm^2 [23]. For semiconducting tubes it seems, somewhat surprisingly, to be even higher [24].

Due to the high conductivity, CNTs are expected to be excellent heat conductors in the axial direction. The weak interaction between the tubes in nanotube bundles and other larger structures, however, makes these structures insulators in the perpendicular directions. The thermal conductivity for an isolated (10,10) SWNT has been predicted to be as high as 6600 W/mK [25]. As the chirality of a nanotube governs all its properties, its effect on the heat conduction has also been studied. For

example, in reference [26], the heat conduction in zigzag nanotubes is presented to be higher than that for chiral tubes. However, one year later another study proposed no chirality dependence at all [27]. Interestingly, a recent experimental study demonstrated that molecule-filled CNTs conduct heat only towards the direction of decreasing mass density [28].

3.4 Applications

Because of their high strength versus mass ratio, CNTs are used for enhancing the mechanical properties of fibers in expensive sports equipment, for example bicycle frames, golf clubs, tennis rackets, ice hockey sticks and bats for Finland's national sport (called *pesäpallo* in Finnish). This is typically achieved by using CNTs to enforce structural polymer (epoxy) composites. The sizes of carbon nanotubes, along with their conductivity, makes them also an interesting option for the tips of scanning probe instruments, such as the atomic force microscope (AFM) and the scanning tunneling microscope (STM) [4]. It is also possible to attach two nanotubes onto a two-electrode AFM tip to be used as nanotweezers [29].

CNTs are shown to have excellent properties for lithium ion batteries, where they can replace the conventional carbon electrodes [30]. Also the possibility of using nanotubes as hydrogen storage media has drawn much attention [4]. Because molecules attached to nanotube surfaces affect the conductance of the tube, CNTs can also be used as sensors. For example, gaseous ambients containing molecules of NO_2, NH_3 and O_2 can be detected with nanotube devices with response times an order of magnitude shorter than that for conventional sensors [31].

CNTs also possess several ideal properties for field emission–based applications: a small diameter along with high electrical conductivity and chemical stability. Prototypes for flat panel displays based on field emission from nanotubes were presented already in 2001 [32]. Also other types of nanotube applications based on the field emission, such as cathode ray lighting devices, have been demonstrated [4]. Semiconducting CNTs can also be used as field effect transistors (FETs) [33; 34; 35; 36]. Especially at low temperatures, CNTs have shown several interesting transport properties [4]. Furthermore, due to their thermal properties, nanotubes can also be used to dissipate heat out from electronic devices. This is especially interesting as molecule-filled nanotubes were recently shown to behave as thermal rectifiers [28].

There are also several possibilities for applications by filling the hollow core of nanotubes. An interesting recent study, for example, presents how CNTs can be used as nanoextruders using electron irradiation [37].

4 METHODS

In a perfect case, we could obtain any needed information with any degree of accuracy from experimental studies. Unfortunately, even the most sophisticated methods have a limited accuracy. For example, studying directly the atomic scale processes during irradiation of nanotubes is experimentally extremely difficult. Therefore, these processes have to be deduced from secondary information, such as macroscopic changes in the irradiated materials, and theoretical approach have to be used to get more insight on the actual processes. All information on a multi-electron system can be obtained with a strict quantum mechanical description by solving the Schrödinger equation. Unfortunately this can be done only for very small systems, and generally different approximations are needed.

Computational methods with different levels of approximations have been utilized in the studies presented in this thesis. The famous Ockham's razor principle: "*entities should not be multiplied beyond necessity* ", introduced by William of Ockham in the late 14^{th}-century, has been applied through all the studies. This means that the simplest possible method yielding the desired accuracy is always used for the given problem. In following, the methods are shortly introduced in the order of increasing number of approximations, starting in section 4.1 with *density-functional theory*, moving on to *tight-binding* method in section 4.2 and *molecular dynamics simulations* in section 4.3, and finally ending in section 4.4 with *kinetic Monte Carlo* method. In section 4.5 the limiting factors of each method are shortly discussed.

4.1 Density-functional theory (DFT)

Most solid state electronic structure calculations are based on density-functional theory (DFT). It relies on the assumption that the many-body wavefunctions Ψ can be replaced by the electron density $n(\mathbf{r})$ as the basic quantity in the quantum mechanical description of the system. Thereby the complexity of the equations can be decreased from $3N$ variables, needed to give the location of all the N particles in the system, to 3. This assumption is based on the Hohenberg-Kohn theorems [38], which state that (a) the ground-state many-body electronic wavefunctions can be one-to-one mapped to the ground state electron density n_0, and (b) this density minimizes the energy of the system. Although the first theorem states that the mapping exists, it does not say anything about its form, and the approximations of DFT methods are done within these mappings.

The most widely used implementation of DFT is the Kohn-Sham method [39], where the problem of the interacting many-body system is reduced to a system of non-interacting electrons in an effective

potential. Within this potential, the electron-nucleus interactions are described with an external field and the Coulombic electron-electron interactions through exchange and correlation terms.

The terms in the Hamiltonian **H** describing the kinetic energy, electrostatic interaction between the electrons and the nuclei, and the electrostatic energy of the electron in the field generated by the total electron density are similar for several electronic structure calculation methods. The exchange-correlation potential $V_{xc}[n](\mathbf{r})$, also included to the Hamiltonian, contains the many-body effects and is unique for DFT.

Solutions to the Schrödinger equation have to be self-consistent in the density given by

$$n(\mathbf{r}) = \sum_{k=1}^{N} |\psi_k(\mathbf{r})|^2, \tag{3}$$

where the sum is over all one-electron spin-orbitals ψ_k having the lowest eigenvalues ε_k. The equations are solved in an iterative self-consistency loop starting with some initial guess for the ground state electron density $n(\mathbf{r})$. As the correct exchange-correlation functional $V_{xc}[n](\mathbf{r})$ is unknown, approximations are needed to solve the equations.

A common way to deal with the electron-electron interactions is the *local density approximation* [40], which is based on exact exchange energy and on fits to the correlation energy for a uniform electron gas. The exchange correlation potential is assumed to depend only on the value of the density in **r**. While the local density approximation is best suited to model bulk materials, other approximations are better for molecules and nanostructures, such as CNTs. To improve on the local density approximation at short distances, the gradients of the electron density can be taken into account with the *gradient expansion approximation*. This leads, however, to unphysical positive contribution at larger distances. In the *generalized gradient approximation*, only the negative contributions are included, and a cut-off is used at larger distances. A large number of different parametrizations based on the approximations exist with varying properties.

As only the valence electrons of the atoms have an effect on the chemistry, the core electrons can be included to a *pseudo potential* which includes both the potential of the nucleus and the screening effect of the core electrons. It has to lead to nearly zero probability for the valence electrons to be close to the nucleus, and describe correctly their behavior after a certain cut-off distance r_C. The implementation of the pseudo potentials leads to a significant computation speed-up by decreasing the number of particles in the system.

DFT calculations utilizing the plane wave basis set VASP code [41] using projector augmented wave pseudo potentials [42; 43] and the generalized gradient approximation [44] have been used to study different defect configurations in publications **I** and **IV**.

4.2 Tight-binding (TB)

The tight-binding method is based on an assumption that the electron states are tightly bound to the nuclei. It consists of a linear-combination-of-atomic-orbitals-(LCAO)–type of approach, in which the atomic states are used as the basis orbitals. The electron states in the tight-binding method are

$$\phi_{\mathbf{k}}(\mathbf{r}) = \sum_p C_p(\mathbf{k})\chi_{p,\mathbf{k}}(\mathbf{r}), \tag{4}$$

where $\chi_{p,\mathbf{k}}(\mathbf{r})$ are the atomic orbitals and $C_p(\mathbf{k})$ are coefficients to be found self-consistently via variational principle method [40] from the generalized eigenvalue problem

$$\mathbf{FC}(\mathbf{k}) = E\mathbf{SC}(\mathbf{k}) \tag{5}$$

for the vector $\mathbf{C}(\mathbf{k})$ with components $C_p(\mathbf{k})$. Equation 5 originates from the Hartree-Fock-Roothaan method [40], and the elements of the Fock matrix **F** can be obtained by fitting to experimental data. **S** is the overlap matrix of the atomic orbitals,

$$S_{pq} = \langle \chi_p(\mathbf{k}) | \chi_q(\mathbf{k}) \rangle, \tag{6}$$

and E consists of the energy eigenvalues ε_k. Within the Slater-Koster approximation [45], the one-electron integrals in the elements of the Fock matrix are approximated with a product of an analytical function depending on the distance between the atoms, and on the overlap of the basis orbitals. This reduces significantly the complexity of evaluating the matrix elements, because originally each element depends on the position of every atom in the system.

Traditionally, the tight-binding method has included some parameters fitted to experimental data. In the density-functional-theory–based tight-binding (DFTB) method [46], however, DFT (see the above section) is used to solve for electron states to be used to calculate the parameters for the overlap and Hamiltonian matrices. The repulsion energy term in the total energy of the system is then fitted to correctly reproduce the results for different structures (for example the C-C dimer). Thereby no experimental data is needed, and the applicability of the method is widened outside the conditions of the experiments used traditionally for fitting. The tight-binding method can also be rigorously derived from DFT [47].

The nonorthogonal DFTB method using the Frauenheim's parametrization [46] is applied both on studying different defect configurations and adatom migration in publication **IV**, and annihilation processes in publication **V**.

4.3 Molecular dynamics (MD)

Classical molecular dynamics (MD) is a method to numerically solve the Newtonian equations of motion for a given system of particles with a known interaction model [48]. It was developed in the late 1950s originally to study the atomic vibrations in molecules [49; 50].

To reduce the computational time needed for the dynamical calculations, the number of free particles in the simulations has to be decreased. A solution used in classical MD is to approximate the atoms as single particles instead of dealing with both nuclei and electrons. This Born-Oppenheimer–approximation [48] is based on the assumption that the electrons move fast enough to reach equilibrium much faster than the nuclei, so that the electronic contribution to the atomic interactions can be neglected.

Although quantum mechanical interactions can be implemented within the MD method (the most famous approach was introduced by Car and Parrinello in 1985 [51]), only classical MD was used in the studies of this thesis. With classical interaction models, the Newtonian equations of motion are integrated over a small time step (typically in the order of 1 fs). For a system with N particles, the potential energy may be divided into terms as

$$\mathscr{V} = \sum_{i=1} v_1(\mathbf{r}_i) + \sum_{(i=1)} \sum_{(j>i)} v_2(\mathbf{r}_i, \mathbf{r}_j) + \sum_{(i=1)} \sum_{(j>i)} \sum_{(k>j>i)} v_3(\mathbf{r}_i, \mathbf{r}_j, \mathbf{r}_k) + \ldots, \tag{7}$$

where the summations are over all particles without counting any pair of particles more than once. The first term presents the external potential and the remaining terms the interactions between the particles.

Several approaches have been taken to solve the equations of motion within the MD method. Typically this is done in a step-by-step fashion using information at time t to calculate the system state at a later time $t+\delta t$. These *finite difference methods* can be further improved with different *predictor-corrector algorithms*.

All MD simulations presented in this thesis have been made with a simulation code PARCAS written by Kai Nordlund [52]. Within this code, the fifth-order Gear predictor-corrector algorithm (Gear5) is utilized (see for example reference [48]) to solve the equations of motion. A variable time step is

used to speed up the computations, while also ensuring a short enough change in time when energetic particles are present.

4.3.1 Inter atomic interaction models

In principle, MD simulations are exact within the Born-Oppenheimer approximation, when the time step is short enough. However, the potential energy of equation 7, arising from the Coulombic and quantum mechanical exchange–interactions, is in practice impossible to calculate exactly for large systems.

One computationally effective method for describing the inter atomic interactions is to use analytical, empirically fitted, potential models. They are typically constructed by first developing a physically motivated functional form, and fitting the free parameters of this functional to reproduce data obtained from experiments or with other numerical methods, such as TB or DFT. When energetic particles force a short time step for the simulations, the interactions can be limited to a small volume around each particle neglecting thus higher-order terms in equation 7.

For metals, a widely used family of interaction models are based on the *embedded-atom method*, originally developed in the 1980s [53; 54]. Within these potentials, the electrons are described with a continuous medium, *jellium*, into which the atoms are embedded. The energy needed to put an atom into its place in jellium is the embedding energy G. The total energy of the system within the embedded atom method becomes

$$E = \sum_i G_i \left[\sum_{j \neq i} \rho_i^a(r_{ij}) \right] + \frac{1}{2} \sum_{i,j(i \neq j)} v_{ij}(r_{ij}), \tag{8}$$

where ρ^a is spherically averaged atom density, v_{ij} describes two-particle interactions and r_{ij} is the distance between atoms i and j.

While the embedded atom method works reasonably well both for noble gases and metals, it does not describe adequately materials with covalent bonds. The *Tersoff-like* potentials have been developed for this purpose [55]. The total energy of the system within these potentials is

$$E = \sum_i E_i = \frac{1}{2} \sum_{i,j(j \neq i)} v_{ij}, \tag{9}$$

where

$$v_{ij} = f_C(r_{ij})[Ae^{-\lambda_1 r_{ij}} - B_{ij}e^{-\lambda_2 r_{ij}}]. \tag{10}$$

E_i is the energy of particle i, v_{ij} is the interaction between particles i and j, r_{ij} is the distance between them, and A, λ_1 and λ_2 are positive constants with $\lambda_1 > \lambda_2$. Parameter f_C defines the cut-off function of the potential. The first term in equation 10 is repulsive, and the second term presents bonding. B_{ij} is a variable including the bond order via a three-body term to take into account the angles between the bonds.

When simulating high-energy events, such as ion irradiation, the interactions at short inter atomic separations are extremely important, because of the high velocity of the particles. While the traditional potential models have been developed usually for simulating near-equilibrium phenomena, they have to be corrected by a smooth joining to a repulsive potential at the shortest distances [56].

4.3.2 Temperature and pressure control

To realistically simulate irradiation events, the heat brought into the structure, dissipated away in a real system, has to be damped out outside the neighborhood of the event to avoid unphysical temperature rise in the system. Therefore, temperature control has to be done in the outer edges of the system, and a large enough system has to be used for the phenomena of interest to occur outside these areas. The Berendsen method [57] of coupling to external temperature bath to dissipate the heat has been used in the MD studies presented in publications **I**-**III**. Although other methods give a better description on thermodynamical ensembles, the Berendsen method is well suited to model an out-of-equilibrium system, such as a nanotube under irradiation. A similar method [57] has been used for pressure control while relaxing the simulated structures. In order to model a much larger structure than possible by simply increasing the system size due to computational limitations, periodic boundary conditions are usually used in irradiation simulations in the directions perpendicular to the irradiation direction.

Classical MD simulations have been used in publications **I**–**III** with Tersoff-like potential by Brenner [58] describing the C-C interaction. A similar potential for B-C-N systems by Matsunaga *et al.* [59] was used in publication **I**, and for C-Si systems by Erhart and Albe [60] in publication **III**. Embedded-atom-method–based potassium potential [61] was used in publication **II**.

4.4 Kinetic Monte Carlo (KMC)

The name of the Monte Carlo methods originates from the famous casino in Monaco, and is due to the fact that these methods rely heavily on random numbers. Kinetic Monte Carlo is a method to simulate processes which occur in a fixed lattice at certain rates [62; 63; 64]. It is well suited to model

the defect migration on solids, the transition rates following the Boltzmann factor including migration energy barrier E_m

$$r_i = \nu_0 e^{-E_m/k_B T}, \tag{11}$$

where ν_0 is characteristic rate which describes the frequency of the events in the system, k_B is the Boltzmann's constant and T is the temperature of the system.

In publication **V**, a new KMC code is introduced for following the diffusion and coalescence of defects on a SWNT. Parameters for the defect migration are obtained from calculations with DFT–based methods. In the *Object KMC* approach taken with this code, the underlaying lattice, on which the defects move, is assumed fixed.

The code utilizes the Bortz-Kalos-Lebowitz–algorithm [62], which proceeds as follows. First, all possible transition in the system are found and the corresponding rates are calculated. After this, one of the transitions is picked randomly according to the rates. This transition is then let to occur, the transition set is updated, and the rates are re-evaluated. This cycle is then continued until a certain end condition is reached. After each transition the system time t is incremented as

$$t = t - \log(u)/R_N, \tag{12}$$

where $u \in [0,1]$ is a random number and R_N is the sum of all the transition rates in the system $R_N = \sum_{i=1}^{N} r_i$.

When the underlaying lattice is rigid and the energetics of the defect migration are known, this allows following the evolution of the defects with a correct time scale [64] if the migration steps are uncorrelated. Using the Bortz-Kalos-Lebowitz–algorithm, only one iteration step is needed to perform each transition, in contrast to many other Monte Carlo methods, making KMC extremely computationally efficient. Therefore it can be used to simulate the time evolution of experimentally observable objects with macroscopic time scales.

As the question of completeness of any greatly simplified model is always somewhat unclear, uncertainties are also introduced to the time scale given by the KMC method. Strictly speaking, using Monte Carlo methods for simulating dynamical processes at all can be questioned, because they describe the order of events rather than the true dynamics of a given system [65]. In fact, there are no means to prove that the dynamics generated by any Monte Carlo scheme would be correct. On the other hand, many case studies have shown that Monte Carlo dynamics can approximate the time dependence of model systems reasonably well. This is further supported by the results discussed in

section 5.3, which are in line with experimental findings for dynamic quantities. Nonetheless, there is a reason to emphasize that care is warranted when Monte Carlo is employed for studies of dynamics.

In the case of defect migration on nanotubes, further complications arise from the flexibility of the tubes in direction perpendicular to the tube axis. Another point is that the prefactor ν_0 is in reality most likely different for different defect types, which is not taken into account in the code presented in publication **V**. There may also be processes which are neglected in the developed model, and the reconstruction of the nanotube atomic structure due to coalescing defects can significantly affect the migration of any near-by defects. However, studies made with the code suggest that the taken approach leads even to a quantitative agreement with experimental results [66].

A KMC method developed by the author for defect diffusion and coalescence on CNTs is introduced in publication **V**. It has been utilized to study the irradiation response of SWNTs at different temperatures under the electron beam of a transmission electron microscope (TEM), and is shown to give results in excellent agreement with experiments.

4.5 Comparison of the computational methods

Methods based purely on quantum mechanical properties of the particles in question, such as DFT, have extreme transferability among the various computational approaches. They can be equally well used to study systems in different phases – same compound as a gas, a liquid or a solid, for example. They can also be used to predict new structures reliably. Solving the Schrödinger equation is, however, such a demanding task that, even with the approximations made within DFT, it can be done only for fast processes (lasting some tens of picoseconds) and involving only a few hundred of atoms. The accuracy of the method depends on the approximations made, and can be continuously increased, at the cost of computational efficiency, by modifying the parameters.

The picture gets more complicated when further approximations are introduced. For example, when TB method is implemented by fitting data from experiments or *ab initio* calculations, the transferability of the method becomes questionable. It is equally difficult to estimate the accuracy of the method without comparison to calculations made with more accurate methods. For DFTB, however, the transferability within geometrical properties of carbon structures has been shown to be similar to DFT [67]. TB method can typically be used to simulate systems with some thousands of atoms and processes lasting up to tens of nanoseconds.

MD method relies heavily on the interaction model used. The analytical interaction models are normally fitted to reproduce a set of known experimental and computational data. Therefore, it depends

crucially on both the quality and the representativeness of this data how well MD describes the system. One clear problem is that the data used to fit the potential is based on known structures, limiting the predictive power of the method. For carbon systems, the Brenner potential [58] has been shown to give a description in good agreement with more accurate methods, especially at low atomic densities [67]. MD can be used to study systems involving millions of atoms up to microsecond regime.

Usually the best understanding of the system is obtained by combining the good properties of all the above-described methods. Time scales or system sizes unreachable even for classical MD with analytical interaction models can be obtained with statistical methods. Object KMC method, for example, can describe the time evolution of defects on a rigid lattice for macroscopic system sizes and realistic time scales, if the energetics of the defect migration and interactions are known. More demanding calculations are needed to obtain the input data for this method, and its accuracy is set by the level of understanding of the underlaying processes.

5 LOW-ENERGY ION IRRADIATION OF NANOTUBES

Although conventionally thought as harmful, irradiation with energetic particles can also have advantageous effects on materials. In the semiconductor industry, for example, ion irradiation is routinely used to introduce dopant atoms into materials to modify their electric properties [68]. In what follows, our computational studies on the possibility to use ion irradiation in a similar manner to tailor the properties of CNTs are presented. Several experimental and computational studies have been made on both electron and ion irradiation effects on different nanotube structures (see a recent review [69] for electron irradiation and references [70; 71; 72; 73; 74; 75] for a few examples on ion irradiation). Most of the studies have concentrated on large-scale structural modifications of the tubes, while only a few studies have considered controlled tailoring of the tube properties with ion irradiation [22; 76]. In the studies presented in this thesis, atomistic simulations have been used to study the possibility of using ion irradiation to ease the route towards applications, especially when large-scale manufacturing of nanotubes with predefined electric properties or good contacts between the tubes and other devices or substrates are needed. The optimum conditions for future experiments are given whenever possible.

The slow-down of ions penetrating to a target is caused by collisions of the ion with electrons and nuclei of the material. As only relatively low irradiation energies ($\leq$ 2 keV) have been used in the studies of this thesis, in order not to destroy the irradiated nanotubes, only the nuclear stopping has been considered. Furthermore, because of the high conductivity of nanotubes, the radiation-induced changes in nanotubes are known to be dominated by the knock-on atom displacements [77].

In the following sections, using ion irradiation to introduce boron, nitrogen and potassium atoms as dopants into CNTs is discussed (original work presented in publications **I** and **II**). After this, a way to improve contacts between nanotubes and substrates with ion irradiation is presented (publication **III**). Finally, the defects introduced to nanotubes due to irradiation, and the time evolution of these defects on nanotube walls (publications **IV** and **V**, respectively) are described.

5.1 Irradiation-assisted doping

As was described in section 3, the electric properties of CNTs are defined by the chirality of each tube, and the as-manufactured nanotube samples contain a mixture of nanotubes with different chiralities. Because of this, a time consuming process of hand-picking and testing the tubes has to precede the fabrication of electronic devices from nanotubes.

Boron and nitrogen can be used for *p* and *n*-type doping of CNTs, respectively, to gain control on their electronic properties. B and N are natural choices for dopants because the atomic radii of these atoms are similar to that of carbon, and they posses one electron less (boron) and more (nitrogen). Further motivation for nitrogen doping arises from the possibility to functionalize [78] nanotubes and to introduce local magnetic moments into them [79] via N impurities.

As an alternative approach, alkali-metal doping has been shown to lead to a change in the electric behavior of nanotube structures. Nanotube ropes, for example, have been reported to become metallic after doping [80; 81]. This happens also for zigzag nanotube–potassium structures with a potassium concentration similar to KC_{48} [82]. In addition, as potassium intercalated fullerene structures are found to be superconductive at temperatures under 19.3 K [83], potassium doping may have an interesting effect on low-temperature behavior of nanotubes. Potassium-doped nanotubes are also of interest as a hydrogen storage medium [84].

Different chemical methods have been considered for the boron and nitrogen doping [85; 86; 87]. With these methods, however, a substantial part of the dopant is usually chemisorbed instead of occupying the substitutional sp^2 configuration in the nanotube atomic network. Furthermore, substitutional reactions seem impossible for nanotubes with diameters less than 8 nm [86], and incorporating B atoms to the atomic network of CNTs has been reported to be problematic [87]. Also potassium doping has been carried out with different methods [35; 80; 81; 84; 88; 89; 90; 91; 92]. A drawback with these methods is that the nanotube structures have to be open-ended, or opened, in order to get the potassium atoms inside, and uniform doping of complex structures is difficult.

Because of the problems in doping CNTs by the chemical methods, other options are worth studying. In publications **I** and **II**, doping of CNTs using ion irradiation has been demonstrated with MD simulations. As the chemical properties and the size of potassium are different than those for boron and nitrogen, also the results of the doping differ significantly.

For boron and nitrogen irradiation, a single-walled armchair carbon nanotube with chiral indices (10,10) was chosen as the target for simulations with the MD method. Ions were aimed at the nanotube in perpendicular direction with respect to the axis of the tube with initial energies of 20–300 eV. After the irradiation, the system was heated up to 1500 K to get rid of spurious metastable configurations. To study the effect of the high-temperature phase on the resulting defect structures, they were visually identified both before and after heating.

To find out the best energy for substitutional doping, the number of neighbors of the dopants was calculated as a function of the irradiation energy. In figure 3 these results are presented for the situation after the high-temperature treatment. As the dopants occupying the substitutional lattice sites in the nanotube have three neighbors, it can be easily deduced from figure 3 that the optimum energy for the substitution is near 50 eV, if the perfect substitution is among the most common defect types where the dopant is three-coordinated. This energy can be understood by the kinetic energy transfer from the ion to the nanotube lattice: within our simulation model it costs about 25 eV to displace a carbon atom, but the ion does not usually hit the carbon atom head-on, thus not giving all its kinetic energy to release the atom. Hence the average energy needed for the displacement increases somewhat, resulting in an average of around 50 eV.

To obtain more detailed picture on the resulting structures after the ion impact, the most prolific structures for both boron and nitrogen were studied also with the DFT method. The four most common structures are presented in figure 4. All these structures were found to be stable both within the MD and the DFT simulations, although the formation of a pentagon in figure 4c was not seen within the MD simulation results.

With the optimum substitution energy of around 50 eV, these defects constitute about 49% and 40% of the structures after the boron and nitrogen irradiation, respectively. If only those dopants are taken into account, which remain in the nanotube after the impact, the probability for the substitution (figure 4a) is about 38% for boron and 65% for nitrogen.

The situation is completely different for potassium doping. Since the potassium atom is much larger than carbon, it can not perfectly replace a carbon atom in the atomic network. Instead, potassium atoms are attracted by the hollow parts of the tube. According to our simulations, only about 2% of potassium atoms are incorporated into the nanotube walls after the irradiation. Furthermore, because

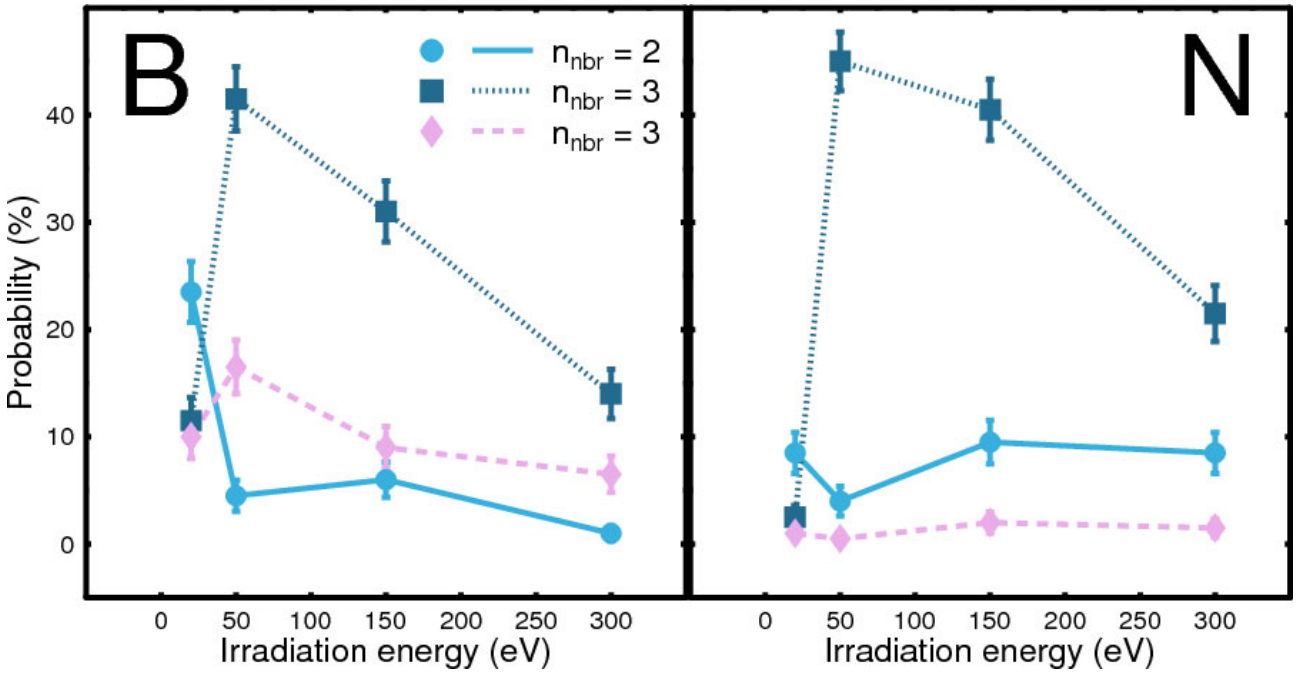

Figure 3: Probability for the boron and nitrogen atoms to have a certain number of neighbors n_{nbr} after the irradiation as a function of the initial ion energy. Only the results after annealing the structures are presented here. This data is from publication **I**.

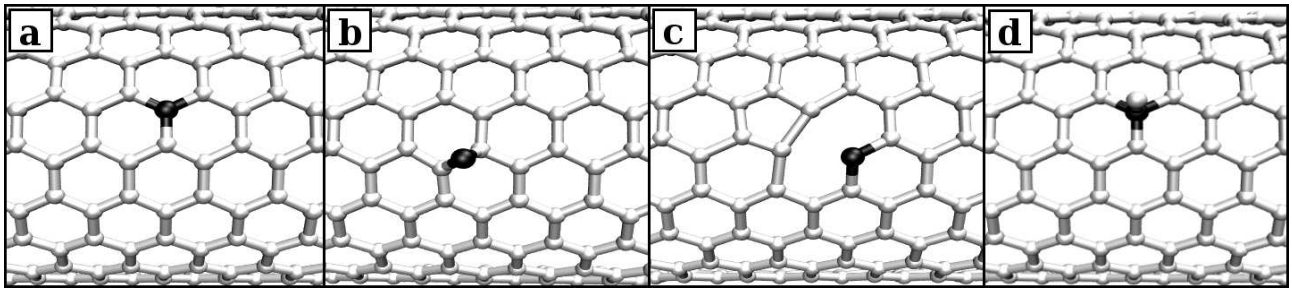

Figure 4: Ball-and-stick presentation of the most prolific defects in a (10,10) SWNT after B/N irradiation. The black atom is the dopant, white atoms are carbon.

of its size, a potassium ion produces more damage to the nanotubes than boron or nitrogen. Therefore, it is preferable to irradiate more robust structures, such as multi-walled nanotubes or carbon peapods[1] with potassium.

To get an estimate on the required irradiation energies for doping multi-walled nanotubes with potassium, we first studied the number of graphitic layers a potassium ion penetrates on average as a function of the ion energy (figure 5). According to figure 5, energies between 50–200 eV are the best for doping a three-walled carbon nanotube (TWNT). To validate this assumption, and to estimate the

[1]Carbon peapod is a structure consisting of a SWNT filled with fullerene molecules.

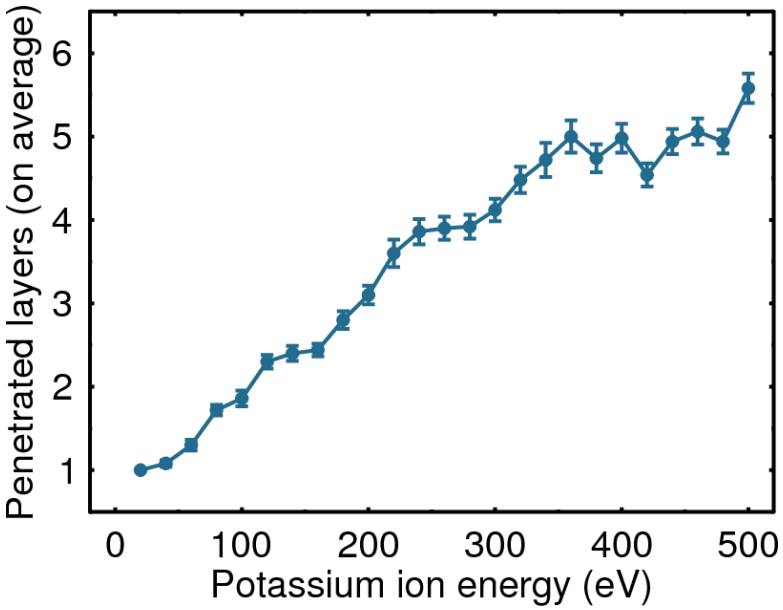

Figure 5: Average number of graphitic layers penetrated by a potassium ion as a function of the initial irradiation energy. This data is from publication **II**.

damage caused during the irradiation, simulations on cumulative irradiation of a TWNT were made. The potassium atoms were found to occupy the hollow parts of the tubes and tend to form small clusters there. The number of introduced clusters divided by the damage is presented in figure 6 as a function of the number of incident K ions for irradiation energies of 60–300 eV. The damage is defined as the ratio between the carbon atoms without graphitic neighborhood and the total number of carbon atoms in the structure.

As figure 6 shows, the energies leading to the maximum number of clusters with the lowest damage for the TWNT are within 60–100 eV. It is evident that ion irradiation can be used to dope CNT structures with potassium. As the probability of obtaining complex defect structures increases with the energy, the lowest possible energy should be used. In the case of carbon peapods, the situation is somewhat better because only one graphitic layer needs to be penetrated. Therefore lower energies can be used for the doping. An example of a carbon peapod structure after potassium irradiation is presented in figure 7.

As a conclusion, ion irradiation is a promising way for substitutional doping of SWNTs with boron and nitrogen, and can also be used to introduce potassium clusters into multi-walled carbon nanotubes and carbon peapods. In fact, the theoretical predictions presented above on nitrogen doping have recently been confirmed experimentally [93], albeit at somewhat higher energies.

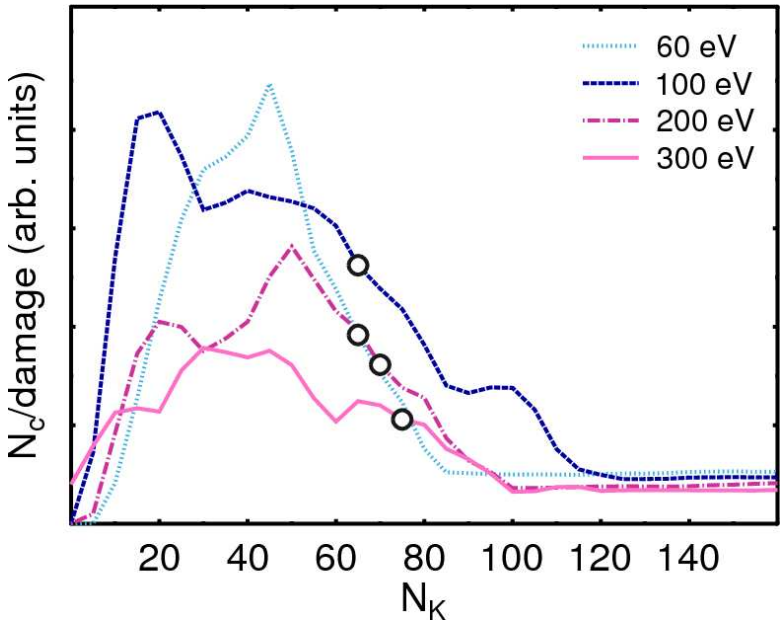

Figure 6: Number of introduced potassium clusters (N_C) divided by the damage as a function of the number of incident K ions (N_K) for irradiation energies of 60 eV, 100 eV, 200 eV and 300 eV. The circles present the points at which the stoichiometry of KC_{48} is reached. The drop in the curves after about 60 potassium ions is due to merging of the clusters together as the potassium concentration increases. The data was originally published in publication **II**.

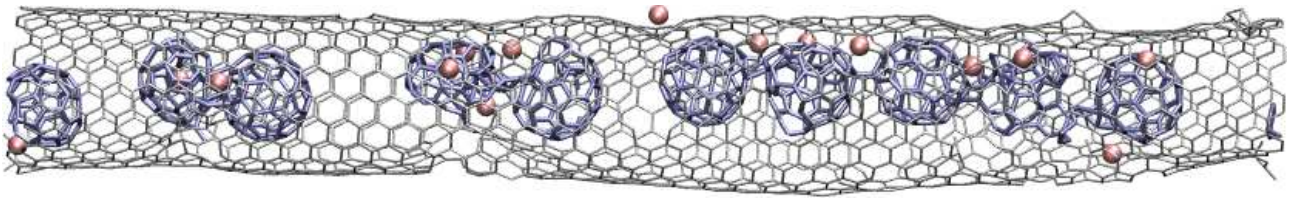

Figure 7: Ball-and-stick presentation of a carbon peapod irradiated with potassium ions with energy of 100 eV. The bonds between the carbon atoms in the nanotube and in the fullerenes are colored differently for clarity. The spheres are potassium atoms.

5.2 Carbon nanotube contacts

Traditionally, nanotube contacts have been created by first fabricating an array of electrodes on a substrate and then depositing nanotubes onto the array. Another possibility is to first deposit the tubes and then place the electrodes over a nanotube, selected for example with an atomic force microscope (AFM).

With these methods, the measured device resistances are usually of the order of 1 MΩ, whereas the intrinsic two-terminal resistance of a metallic CNT is half the quantum of resistance $1/2G_0 = h/4e^2 \approx$

6.5 kΩ [4]. The difference of two orders of magnitude between these values is usually related to the contact resistance at the nanotube-electrode interfaces. Lower contact resistances have been obtained for example by evaporating metals on CNTs on substrates [94]. The lowest measured resistances have been as low as ∼10 kΩ. Also other approaches have been used to obtain similar values. However, even with evaporated electrodes, roughly one of every four contacts is not working properly. Because of this, the contacts have to be tested every time causing a significant amount of extra work. In addition, when using a multi-walled nanotube, these methods contact only the outermost wall to the electrodes, whereas contacting all the layers should give a clear increase in the conductance.

Focused electron irradiation has been used to solve these problems by improving the contacts. A significant decrease of the originally high contact resistances has been reported ($>$ 100 MΩ $\rightarrow$ 30 kΩ) [95]. Because ion guns are more frequently found in today's semiconductor device facilities, when compared to scanning-electron microscopes (SEM) used in the study of reference [95], it could be preferred by the semiconductor industry to use ion irradiation in a similar manner. Furthermore, using ion irradiation and protective masks outside the contact areas, the requirements for mass production can be approached, because the structure can be uniformly irradiated.

The question of charge transfer between CNTs and metal electrodes has recently also been theoretically addressed [96]. The highest transfer was surprisingly found to occur with a weak contact between the nanotube and the metal electrode, but with as long contacts as possible. However, the study presented in reference [96] concerns pristine nanotubes and crystalline metals. As the results with the focused electron and ion beams indicate, the situation is somewhat different when the nanotube and the metal electrode have been welded together with energetic impacts.

Preliminary results from a study on ion irradiation of a nanotube on SiO_x surface under evaporated gold contacts, with the uncovered part of the nanotube protected with a resist layer, are promising [97]. However, more experiments have to be made in order to make reliable interpretations on the obtained results. An example of the structure used in these experiments is presented in figure 8 both before and after the irradiation.

In addition to enhancing the contacts between CNTs and metal electrodes, it can be useful to contact tubes also to semiconductor materials, especially to silicon. Although the possibility of redesigning the existing semiconductor devices to be made of carbon materials, such as nanotubes, has been discussed [2], silicon can not be replaced in the very nearest future. A possible route towards carbon-based electronics goes via integrating the existing silicon technology with CNTs. One possible direct application for a nanotube–silicon system could be heat dissipation out of silicon devices using nanotubes connected directly to the device, utilizing the excellent heat conductivity of nanotubes [25].

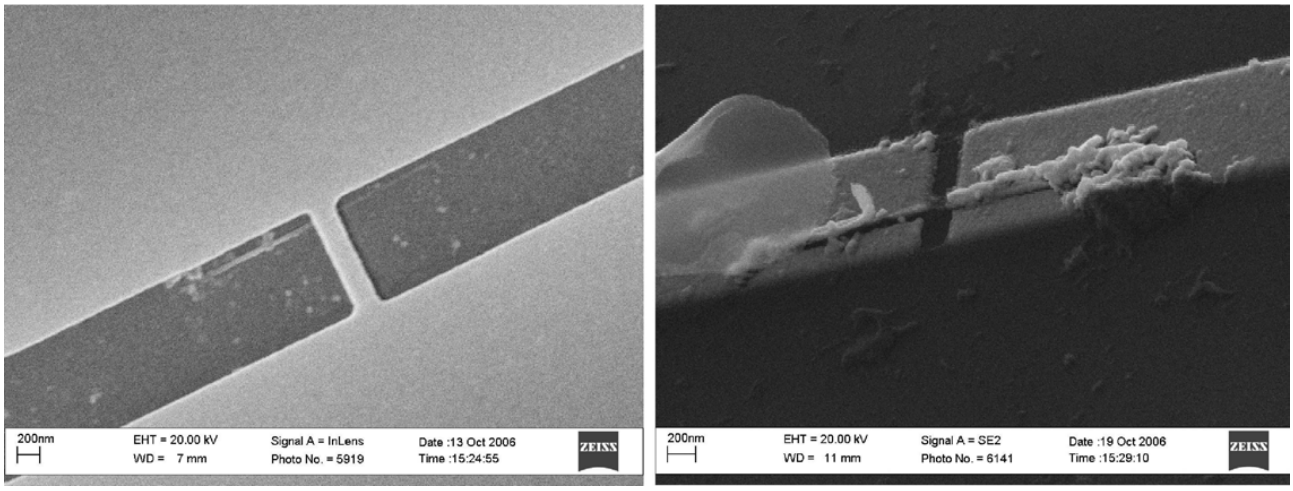

Figure 8: Scanning electron microscope (SEM) images of the irradiated nanotube–electrode–resist structure before (left) and after (right) the irradiation. The images are from different samples. Images are courtesy of Lorenz Lechner, Low Temperature Laboratory, Helsinki University of Technology, Finland.

Furthermore, if nanotubes loaded with molecules can be used as thermal rectifiers as was recently demonstrated [28], a multitude of new applications can emerge.

The study presented in publication **III** shows how ion irradiation can be used to enhance the nanotube–silicon contact. A structure with a trench in the substrate was studied to demonstrate at the same time how the geometry of the system can be designed to avoid unnecessary destruction of those parts of the nanotube which do not need to be damaged. This is possible due to the difference in damage production between suspended nanotubes and tubes on substrates [98; 99], caused by the back-scattering and recoils from the substrate. The structure used in this study is presented in figure 9.

Irradiation of this structure with carbon, silicon and neon ions was studied with the MD method using irradiation energies of ≤ 2 keV. As the result of the irradiation, a clear increase of the number of new C-Si bonds in the contact areas $[0.5 - 0.9 \times (10^{14}\ \text{ions/cm}^2)^{-1}]$ was found. Also the increase in the binding energy between the structures was estimated. It is presented in figure 10 divided by the irradiation dose as a function of the ion energy for all the studied ions.

Because the structure was uniformly irradiated, some damage was also created in the suspended part of the nanotube. Fortunately, at least for the lowest irradiation energies, most of the produced defects are single vacancies [98]. As these defects are mobile with migration energies of about 1.3 eV (see the following section), the damage production can be decreased by increasing the irradiation temperature. If the ion beam current is kept low enough, the defects can migrate to the damaged parts of the

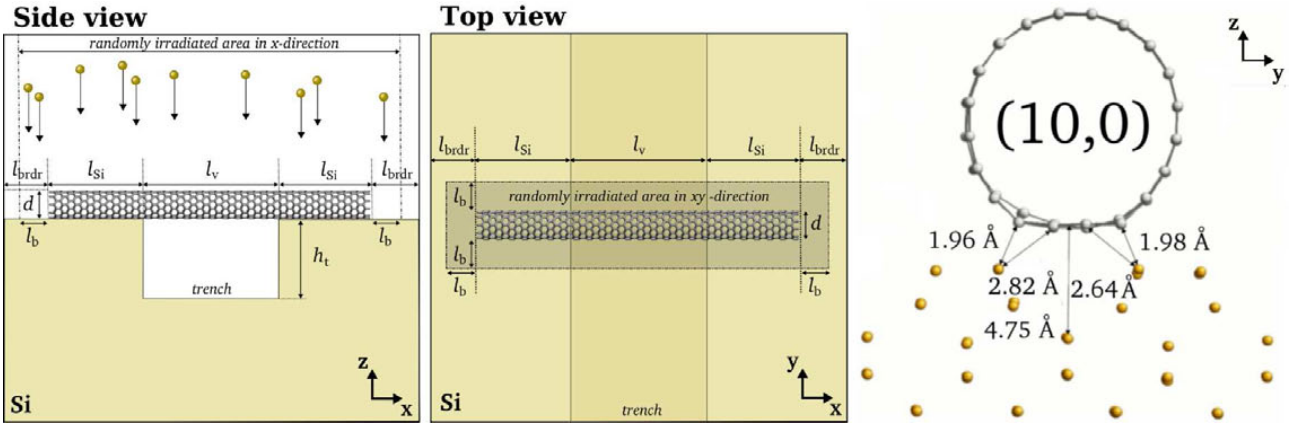

Figure 9: Schematic presentation of the irradiated structure in two directions and presentation of the atomic structure of the minimum-energy configuration for a (10,0) SWNT in between the dimer ridges on the silicon surface in the third direction. All panels are from publication **III**.

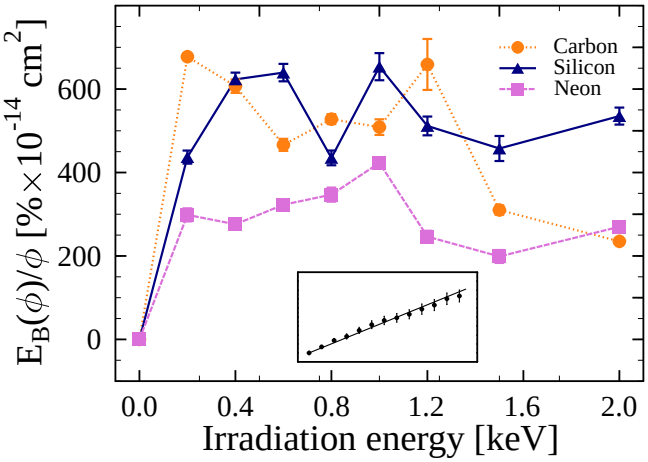

Figure 10: Increase in the binding energy (E_B) between the tube and the substrate divided by the irradiation dose (ϕ) for different ions as a function of the initial ion energy. The inset shows an example of the binding energy/irradiation dose data from which the data presented in the graph were obtained with linear fits. The graph is from publication **III**.

tube, where they are likely to recombine with other defects. Although the increasing temperature also enhances the healing of the contact areas, it is unprobable that the contacts retain their original structure if the temperature increase is kept modest, allowing the welding of the nanotube to the substrate.

With increasing energies also the number of immobile higher-order defects increases. As an example, figure 11 presents a part of the structure after carbon irradiation with an energy of 2 keV and an

irradiation dose of 0.55×10^{14} ions/cm^2.

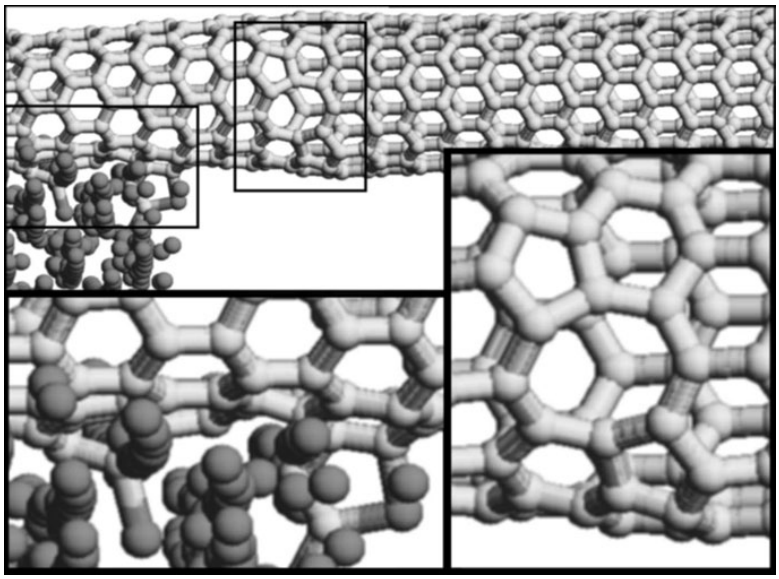

Figure 11: Ball-and-stick presentation of a (10,0) SWNT on a Si-substrate after carbon irradiation with an energy of 2.0 keV and irradiation dose of 0.55×10^{14} ions/cm^2. Light spheres present carbon and dark spheres silicon atoms. Irradiation has created a (5-8-5) divacancy structure to the suspended part of the tube (right-hand-side zoom-in), and also new bonds are evident between the structures (left-hand-side zoom-in). This figure is from publication **III**.

The results indicate that ion irradiation can be used to enhance the contacts between CNTs and different kinds of substrates. Specifically, ion irradiation-induced welding of a SWNT to a silicon surface was demonstrated using MD simulations with an example geometry to decrease the unwanted damage in some parts of the nanotube. Typical increase on binding energy between the nanotube and the silicon substrate was found to be about 100–400% with moderate irradiation doses. If the irradiation energies and beam currents are kept low, and the irradiation is performed at an elevated temperature, the contacts can be enhanced without intolerable damage caused to the nanotube.

5.3 Irradiation response

The most typical irradiation-induced defects in CNTs are atomic vacancies along with interstitial carbon atoms [98]. After a carbon atom is displaced from its position in the nanotube atomic network, it is likely to hit the surface of the tube on the other side. If the energy of this displaced atom is not high enough to kick out another carbon or to escape from the structure, it gets attached to the lattice as an adatom (interstitial). Because of the curvature of the tubes, there are two different surfaces for the adatom to occupy. It can either be on the inside surface in an *endohedral* position or on the

outside surface in an *exohedral* position. Also other defect types, such as the Stone-Wales defect [100] related to a switched bond, can be found after irradiation. However, the energy barrier for a Stone-Wales defect to transform back to perfect lattice has been shown to be very low with adatoms present in the structure [101], which is usually the case in irradiation experiments.

The minimum-energy configuration for an adatom is over a carbon-carbon bond perpendicular to the tube axis. For a vacancy the structure rearranges by decreasing the distance between two of the remaining atoms to create a weak bond forming a pentagon. The third atom remains under-coordinated. For illustrations of these structures and description of their properties see references [102] and [103], respectively. As the average migration energy barriers for these defects are, on a relatively small SWNT, of the order of 0.5 eV (adatom) [102] and 1.3 eV (vacancy) [103], it can be easily deduced that they are both mobile at experimentally interesting temperatures. For example, at a temperature of 600°C, the diffusion rate for an adatom on a nanotube wall can be estimated with equation 11 to be

$$r_i = \nu_0 e^{-0.5 \text{ eV}/k_B T} \approx 5.2 \times 10^9 \text{ s}^{-1} \tag{13}$$

and for vacancy diffusion

$$r_v = \nu_0 e^{-1.3 \text{ eV}/k_B T} \approx 1.3 \times 10^5 \text{ s}^{-1}, \tag{14}$$

when $\nu_0 \approx 4 \times 10^{12}$ s^{-1} is the vibrational frequency for a carbon atom on a nanotube [102] and k_B is Boltzmann's constant. Hence not only the amount of the produced defects, but also their migration is important from the experimental point of view. At room temperature the rates are several orders of magnitude lower.

As the defects are mobile, an obvious question is what happens when they meet. For a single vacancy and an adatom meeting each other, the simplest assumption is to expect annihilation, after which the remaining structure is that of a perfect nanotube. However, in reality the situation is not this simple, because the recombination does not always lead to the perfect structure [66]. Similar behavior has also been seen for graphite [104]. However, as is discussed in publication **V**, this can be expected to be important only at the lowest temperatures.

Although some studies have been made on properties of carbon dimers on nanotubes [105], it is not obvious what happens when two interstitial atoms meet. The most naïve picture is to assume that there is no significant agglomeration of interstitial atoms on CNTs when the adatom concentration is low, as this is not seen in TEM studies even with high currents [106]. Comparison between results with the KMC method presented in publication **V** and experiments seem to validate this assumption. For vacancies, however, the situation is completely different. Several multivacancy configurations were

studied with the DFTB method in publication **IV** in order to find the minimum-energy structures forming via coalescence of single vacancies. Also a weak but long-ranged interaction between single vacancies was found within these studies, and the DFT method and an empirical force model (a Tersoff-like inter atomic potential, see section 4.3.1) were used to estimate the electronic and strain field–related contributions on this interaction.

The agglomeration of vacancies to form multivacancy structures was found to be promoted by the weak long-range interaction, and also by the energy gained within the coalescence (see figure 12). However, as is shown in publication **IV**, the multivacancy structures tend to have an upper limit of five removed atoms. Defects larger than this easily split into smaller multivacancies to more efficiently reconstruct the atomic network of the tube, at least in isolated SWNTs with small diameters (see the structure of V_6(5-7-6-7-5)$^{\|}$ in figure 13).

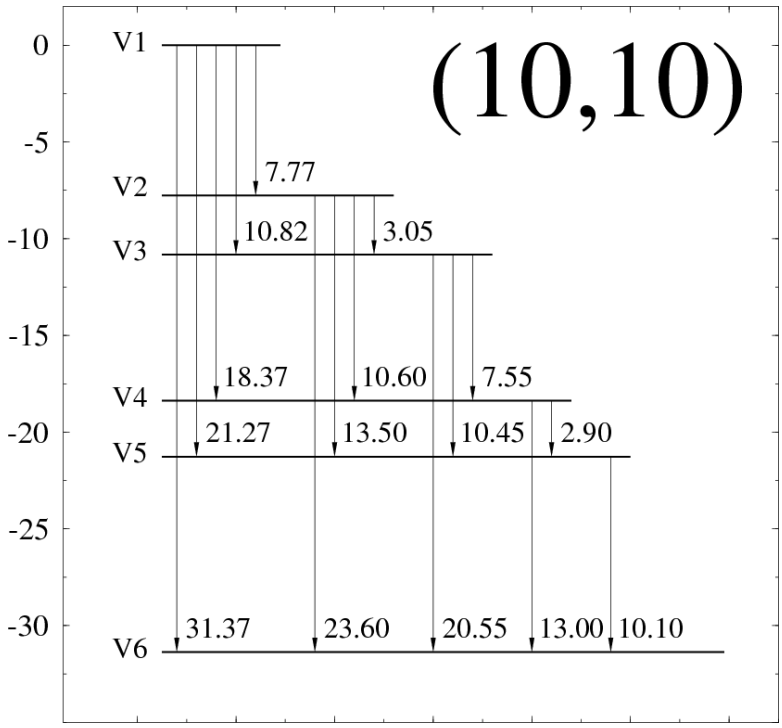

Figure 12: Energies (in eV) gained while forming multivacancies from separated single vacancies in a (10,10) SWNT. The data is from publication **IV**.

Figure 12 clearly shows that the energetically most favored configurations have an even number of missing carbon atoms; $\sim$7.5 eV is gained when one single vacancy is added to a multivacancy with an odd number of missing atoms, whereas less than 3.0 eV is released when the original defect is even-numbered. The minimum-energy configurations for multivacancies with 2–6 removed atoms are presented in figure 13 for a (10,10) SWNT and the related energies are listed in table 1.

Table 1: Formation energies of the vacancy structures on a (10,10) SWNT calculated with the DFTB method. Values in parentheses give the number of atoms in carbon rings in defects. Subscripts show the number of dangling bonds in each ring. Orientations of defects ('parallel' $\parallel$ and 'perpendicular' $\perp$) are given as the orientation of the longest chain of missing atoms in each defect with respect to the nanotube axis. The data in the table is from publication **IV**.

Defect structure	$E^{(f)}$ (eV)
$V_2(5\text{-}8\text{-}5)^{\parallel}$	5.25
$V_3(5\text{-}10_1\text{-}5)^{\parallel}$	8.70
$V_4(5\text{-}7\text{-}7\text{-}5)^{\parallel}$	7.67
$V_4(5\text{-}5\text{-}5\text{-}9)$	10.32
$V_5(5\text{-}5\text{-}5\text{-}11_1)$	11.27
$V_5(5\text{-}14_3\text{-}5)$	12.55
$V_6(5\text{-}7\text{-}6\text{-}7\text{-}5)^{\parallel}$	7.68
$V_6(18_6)$	17.21

It is interesting to note that several of the minimum-energy structures differ from the ones calculated for graphite. This is due to the fact that in graphite the reconstruction of the atomic network can occur in two dimensions, whereas in nanotubes only the circumferential direction is available due to the stiffness of the tubes in the axial direction.

The reason for the lower formation energies of the even-numbered multivacancies is obvious from the structures presented in figure 13: all atoms in these defects are three-coordinated and remain therefore at least partially sp^2-hybridized, whereas some under-coordinated atoms with *dangling bonds* are present in the odd-numbered ones. The effective reconstruction of the atomic network of CNTs is the main reason for the experimentally observed shrinkage of the tubes under electron irradiation with high currents [107]. It also explains the pressure build-up in multi-walled nanotubes acting as nanoextruders for encapsulated metal particles [37].

Using the above information with the diffusion energies for the defects [102; 103] as input data for the KMC method (see section 4.4), we can follow both the time evolution of defected nanotubes and their response to irradiation at time scales unreachable by any other method. In publication **V** a new simulation code based on the KMC method is introduced and utilized in studying the temperature dependence of the irradiation response of SWNTs. The most important processes implemented within the code are presented in figure 14.

As a test for our code, we used it to study the behavior of different SWNTs under a TEM beam at several temperatures. The defect concentrations for a (10,10) SWNT are presented in figure 15. In perfect agreement with the experiments [69; 108], we found that at temperatures higher than $\sim 300^{\circ}$C, the self-healing process of CNTs is fast enough for the irradiation-induced defects to annihilate *in situ*

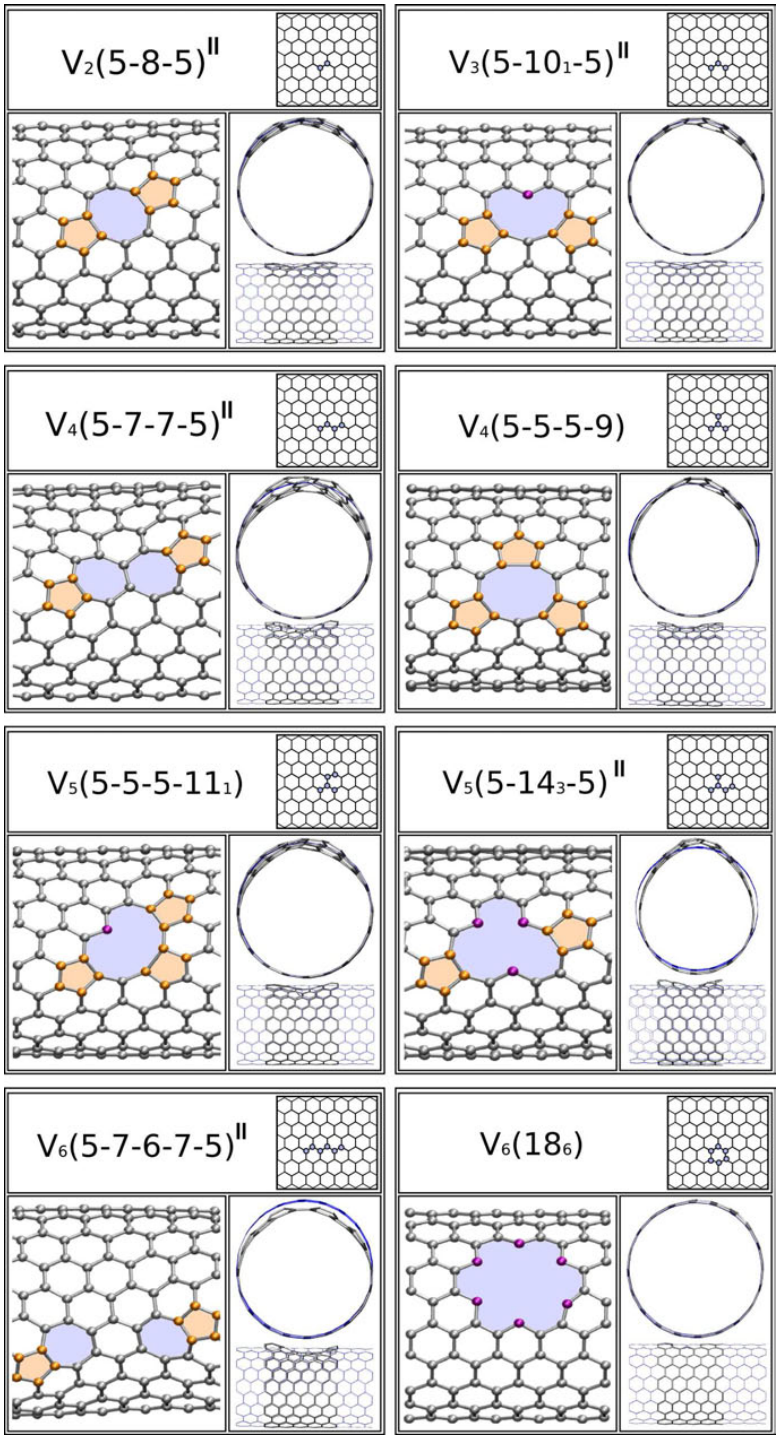

Figure 13: Lowest energy structures of multivacancies in a (10,10) SWNT with 2–6 missing atoms. Formation energies of these defects are given in table 1. The figure is from publication **IV**.

nearly perfectly. The results on the times needed to cut a nanotube with the TEM are also similar to the experimental values [69; 108], although experimental uncertainties related to the pretreatment of the tubes makes a direct comparison difficult. After 10 s of irradiation a vacancy concentration of 0.1%

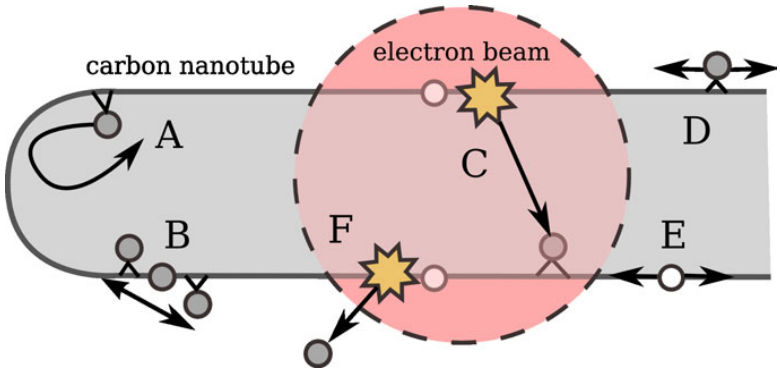

Figure 14: Schematic representation on the most important processes included in our model. (A) A diffusing endohedral adatom is reflected back from a cap. (B) Endohedral-exohedral transformation of an adatom through the exchange mechanism. (C) Electron impact creating a defect pair (white sphere - a vacancy, gray sphere - an adatom) by displacing a carbon atom. (D and E) Adatom and vacancy migration, respectively. (F) Creation of a vacancy by sputtering the displaced atom. Figure is from publication **V**.

is found in a (10,10) SWNT at temperature as high as about 530°C (see figure 15). Our simulations show that a vacancy concentration of 1% leads to a decrease in the cutting times by a factor of six. Hence the results depend heavily both on the purity of the samples and on their treatment before the experiments. Furthermore, as is presented in publication **V**, the chirality of the tubes is also important for the irradiation response.

According to figure 15, there is a temperature range slightly above room temperature ($\sim 130-230$°C) at which the heating can also have a negative effect on the self-healing. This is most likely due to the increase in vacancy mobility making it easier for them to find each other and to form immobile multivacancy structures. However, only after about 300°C they are fast enough to escape the irradiated area to avoid rapid destruction of this part of the tube. Therefore, to ensure effective self-healing, the temperature for the experiments should be at least 300°C, although some defects will remain in the structures even at the highest studied temperatures.

The code can be used for a wide variety of studies involving defected CNTs or nanotubes under electron or ion irradiation. It can also be applied to evaluate the importance of different processes on nanotube growth. Further improvements of the code (to include for example the correct multivacancy structures) are underway.

As a conclusion, the studies presented in publications **IV** and **V** show that although irradiation damages CNTs while used for tailoring their properties, the damage production can be lower than could be simply assumed *a priori* or by MD simulations. For this purpose, the beam currents and irradiation energies should be as low as possible and the experiments should be carried out at a temperature higher

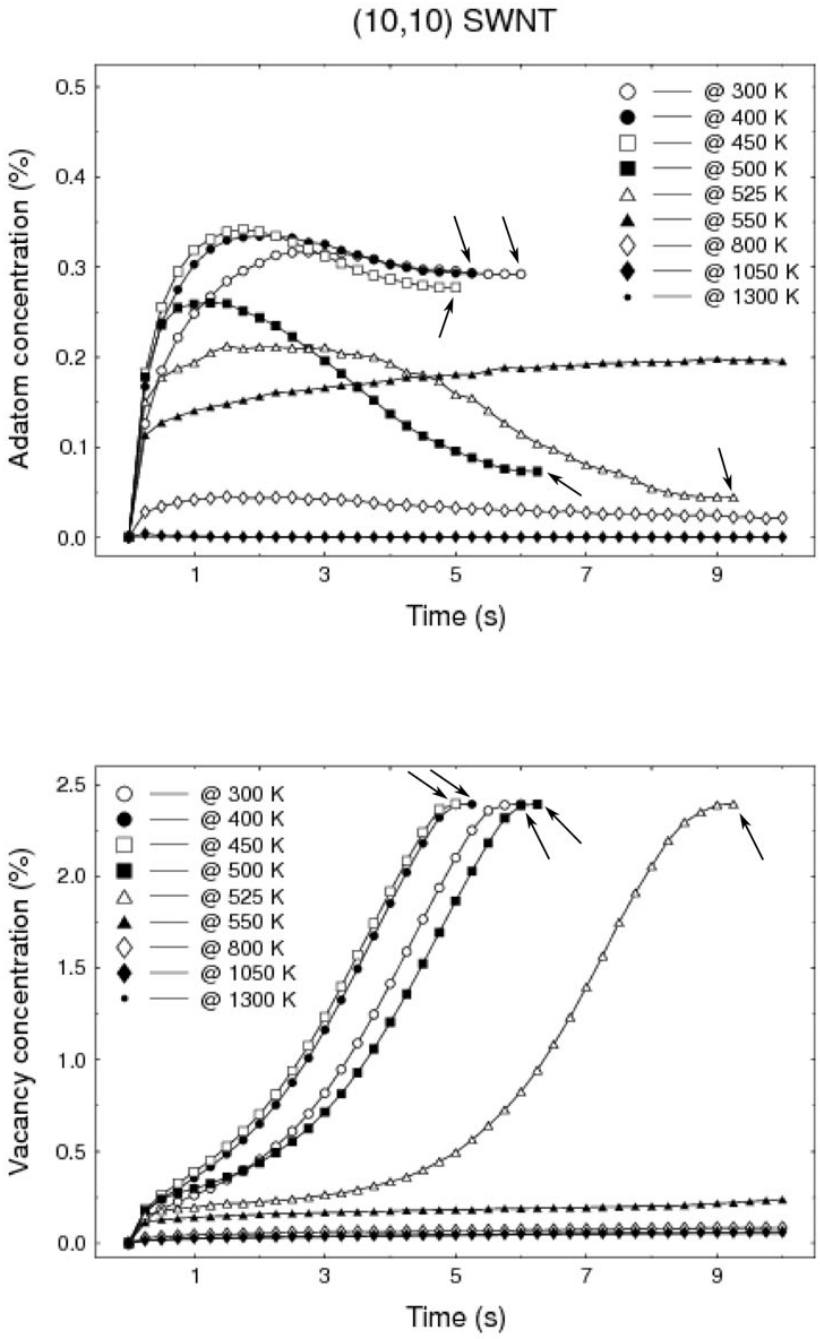

Figure 15: Adatom and vacancy concentrations in an irradiated (10,10) SWNT as a function of time at different temperatures under a TEM beam causing 1 dpa/s (current of $\sim 10^4$ A/cm^2). The arrows indicate the break-up points of the tubes. The presented data is averaged over several simulations (up to 40), and the standard error is typically of the order of 10 % of the values. Figure is from publication **V**.

then or equal to 300°C. Furthermore, even when complex defects are introduced to the structures, the atoms tend to remain three-coordinated whenever possible, thereby retaining, at least partially, the exciting properties of the pristine nanotubes.

6 CONCLUSIONS

In this thesis, atomistic simulations with different levels of theory have been utilized to demonstrate how ion irradiation can be used to tailor properties of CNTs and to ease the route towards large-scale manufacturing of CNT applications for electronics. The dynamical processes have been studied with the MD method using analytical interaction models, while more accurate DFT–based methods have been used to investigate the stability and properties of irradiation-induced defect structures on nanotube walls. Finally, a new KMC code has been introduced and applied on studying the irradiation response of nanotubes at different temperatures under a TEM with realistic system sizes and at time scales of several seconds.

MD simulations were used to show that ion irradiation is able to introduce substitutional boron and nitrogen impurity atoms to SWNTs with remarkably high probabilities with the optimum irradiation energy of about 50 eV. With this energy, it is possible to get one third of boron and two thirds of nitrogen atoms into these positions, if only those dopant atoms are counted which remain in the nanotube structure after the ion impact. The stability of the structures resulting from the irradiation events was confirmed by DFT calculations. The amount of substitutional dopants was shown to be likely to increase from the presented values via defect migration, because the dopants, at least boron, were found to be attached to the nanotube surface only weakly when not occupying the substitutional position.

Potassium doping of MWNTs was also presented. The large size of a potassium atom, as compared to carbon, boron or nitrogen, hinders substitutional doping. In fact, less than 2 % of the potassium dopants were found to be incorporated into the atomic network of the nanotube after irradiation. However, as there are large hollow parts inside nanotubes, the potassium atoms were found to form small clusters in these areas both in multi-walled nanotubes and in carbon peapods. For a three-walled nanotube the optimum irradiation energy for potassium doping was found to be about 100 eV.

Enhancement on the contact interaction between CNTs and different substrates was also discussed. Specifically, MD simulations were used to show that ion irradiation can significantly increase the number of covalent carbon-silicon bonds between a CNT and a silicon substrate. The tube was deposited over a trench to make use of the differences in defect production between suspended nan-

otubes and those on substrates. Typical increases in the number of new covalent bonds was found to be $0.5 - 0.9 \times (10^{14}$ ions/cm$^2)^{-1}$ and the binding energy was found to increase about $100 - 400$ % for moderate energies. All simulated ions (carbon, silicon and neon) were shown to be able to enhance the contacts, but the effect is more significant for the heavier carbon and silicon ions. When the energy and ion used for the irradiation are correctly chosen (for example carbon with an energy of 0.2 keV), the damage caused to the suspended part of the nanotube should be tolerable.

In order to understand the behavior of the irradiation-induced defects in nanotubes, the vacancy properties were studied with the DFTB method. It was used to find the minimum-energy structures of multivacancies with up to six missing atoms on the wall of a (10,10) SWNT. Defects with six or more missing atoms were found to be unlikely to form via vacancy coalescence. In the minimum-energy structures all the atoms remain three-coordinated via structure reconstructions with a requirement of an even number of missing atoms. The vacancies tend to align chain-like in the axial direction of the tube to ease the reconstruction within the multivacancy structures. A weak but long-ranged interaction was also found within the calculations. Further studies with DFT and an empirical interaction model showed that this interaction is a combination of electronic degrees of freedom and mechanical strain.

For studying the irradiation response of SWNTs at different temperatures, a new KMC code was developed. The input parameters for the defect diffusion, such as the defect structures and the energetics related to the diffusion, are obtained from DFT–based calculations. The code allows either following the irradiation process or the time evolution of defected nanotubes with realistic system sizes (up to several μm) at time scales of several seconds. As a test, the code was utilized on studying the nanotube behavior under a TEM beam. The self-healing process of nanotubes was found, in perfect agreement with experiments, to be effective enough to nearly perfectly annihilate the irradiation-induced defects at temperatures $\geq 300^\circ$C. Also the results on times needed to cut a nanotube with the TEM were similar to experimental values, although experimental uncertainties make the comparison difficult. As a surprise, we also found that at a certain temperature range slightly above the room temperature ($\sim 130 - 230^\circ$C) heating can also have a negative effect on the self-healing process of nanotubes. Therefore, nanotube imaging and irradiation should always be carried out at temperatures of at least 300°C.

To conclude, ion irradiation was shown to enable modifying the properties of CNTs in a controlled manner. Although some damage is always caused to the structures during the irradiation process, our simulations showed that the damage can be nearly perfectly annealed *in situ* (if the irradiation temperature is $\geq 300^\circ$C). Nanotubes were further found to efficiently reconstruct the lattice to ensure a graphitic neighborhood for all atoms also in the presence of complex defects. Overall, our results

are very promising for using ion irradiation to tailor properties of CNTs and to improve CNT contacts in large-scale manufacturing processes.

ACKNOWLEDGMENTS

I wish to thank the head of the Department of Physical Sciences at the University of Helsinki, Professor Juhani Keinonen, as well as the head of the Accelerator Laboratory, Professor Jyrki Räisänen, for providing the facilities both for my studies and for conducting the research presented in this thesis at my disposal.

A very warm thank you goes to my supervisor for the past three years, Professor Kai Nordlund, both for introducing me to the subjects and most of the methods discussed in this thesis, and for being an encouraging example of a forever-enthusiastic scientist equally excited about every new finding which he encounters. I am no less in debt to my second supervisor, Docent Arkady Krasheninnikov, whom I have to thank for nearly always bringing my head back from the clouds. Him I would also like to thank for teaching me the most I know about being a scientist.

It would be unfair to not thank here also everyone who contributed to the studies presented in this thesis, or to not acknowledge the effect of having such a collection of great people as colleagues as I had during my years at the Accelerator Laboratory. Especially, I wish to thank Kristoffer, Carolina and Niklas – I loved every moment with you. May there be many more to come.

Finally, there are no words to describe my gratitude towards my dear wife Stella. Without her I would not have been able to finish this thesis. In fact, I am in doubt whether I would have ever become a scientist without her.

Once more, thank you all.

Darmstadt, Germany, February the 26th, 2007
Jani Kotakoski

References

1. S. Iijima, *Helical microtubules of graphitic carbon*, Nature **354**, 56 (1991).

2. P. G. Collins and P. Avouris, *Nanotubes for electronics*, Scientific American **52(5)**, 62 (2000).

3. L. X. Zheng, M. J. O'Connel, S. K. Doorn, X. Z. Liao, Y. H. Zhao, E. A. Akhadov, M. A. Hoffbauer, B. J. Roop, Q. X. Jia, R. C. Dye, D. E. Peterson, S. M. Huang, J. Liu, and Y. T. Zhu, *Ultralong single-wall carbon nanotubes*, Nat. Mater. **3**, 673 (2004).

4. M. S. Dresselhaus, G. Dresselhaus, and P. Avouris (Eds), *Carbon Nanotubes, Synthesis, Structure, Properties and Applications* (Springer, Berlin, 2001).

5. R. H. Baughman, C. Cui, A. A. Zakhidov, Z. Iqbal, J. N. Barisci, G. M. Spinks, G. G. Wallace, A. Mazzoldi, D. De Rossi, A. G. Rinzler, O. Jaschinski, S. Roth, and M. Kertesz, *Carbon Nanotube Actuators*, Science **284**, 1340 (1999).

6. A. Hashimoto, K. Suenaga, A. Gloter, K. Urita, and S. Iijima, *Direct evidence for atomic defects in graphene layers*, Nature (London) **430**, 870 (2004).

7. K. Urita, K. Suenaga, T. Sugai, H. Shinohara, and S. Iijima, *In Situ Observation of Thermal Relaxation of Interstitial-Vacancy Pair Defects in a Graphite Gap*, Phys. Rev. Lett. **94**, 155502 (2005).

8. A. Oberlin, M. Endo, and T. Koyama, *Filamentous growth of carbon through benzene decomposition*, J. Cryst. Growth. **32**, 335 (1976).

9. H. W. Kroto, J. R. Heath, S. C. O'Brian, R. F. Curl, and R. E. Smalley, *C_{60}: Buckminsterfullerene*, Nature **318**, 162 (1985).

10. E. Schröder and P. Hyldgaard, *Van der Waals interactions of parallel and concentric nanotubes*, Mat. Sci. Eng. C **23**, 721 (2003).

11. S. Iijima and T. Ichihashi, *Single-shell carbon nanotubes of 1-nm diameter*, Nature **363**, 603 (1993).

12. D. S. Bethune, C. H. Kiang, M. S. de Vries, G. Gorman, R. Savoy, J. Vazquez, and R. Beyers, *Cobalt-catalysed growth of carbon nanotubes with single-atomic-layer walls*, Nature **363**, 605 (1993).

13. R. E. Smalley, Y. Li, V. C. Moore, B. K. Price, R. Colorado, H. K. Schmidt, R. H. Hauge, A. R. Barron, and J. M. Tour, *Single Wall Carbon Nanotube Amplification: En Route to a Type-Specific Growth Mechanism*, J. Am. Chem. Soc. (2006), in press.

14. A. G. Nasibulin, P. V. Pikhitsa, H. Jiang, and E. I. Kauppinen, *Correlation between catalyst particle size and single-walled carbon nanotube diameters*, Carbon **43**, 2251 (2005).

15. E. Gregan, S. M. Keogh, A. Maguire, T. G. Hedderman, L. O. Neill, G. Chambers, and H. J. Byrne, *Purification and isolation of SWNTs*, Carbon **42**, 1031 (2004).

16. E. W. Wong, P. E. Sheehan, and C. M. Lieber, *Nanobeam Mechanics: Elasticity, Strength, and Toughness of Nanorods and Nanotubes*, Science **277**, 1971 (1997).

17. R. H. Baughman, A. A. Zakhidov, and W. A. de Heer, *Carbon Nanotubes – the Route Toward Applications*, Science **297**, 787 (2002).

18. Y. Fan, B. R. Goldsmith, and P. G. Collins, *Identifying and counting point defects in carbon nanotubes*, Nat. Mater. **4**, 906 (2005).

19. M. Sammalkorpi, A. V. Krasheninnikov, A. Kuronen, K. Nordlund, and K. Kaski, *Mechanical properties of carbon nanotubes with vacancy-like defects*, Phys. Rev. B **70**, 245416 (2004).

20. N. Hamada, S.-I. Sawada, and A. Oshiyama, *New One-Dimensional Conductors: Graphitic Microtubules*, Phys. Rev. Lett. **68**, 1579 (1992).

21. L. Chico, L. X. Benedict, S. G. Louie, and M. L. Cohen, *Quantum conductance of carbon nanotubes with defects*, Phys. Rev. B **54**, 2600 (1996).

22. G. Gómez-Navarro, P. J. De Pablo, J. Gómez-Herrero, B. Biel, F. J. Garcia-Vidal, A. Rubio, and F. Flores, *Tuning the conductance of single-walled carbon nanotubes by ion irradiation in the Anderson localization regime*, Nat. Mater. **4**, 534 (2005).

23. Z. Yao, C. L. Kane, and C. Dekker, *High-Field Electrical Transport in Single-Wall Carbon Nanotubes*, Phys. Rev. Lett. **84**, 2941 (2000).

24. Y.-F. Chen and M. S. Fuhrer, *Current-carrying capacity of semiconducting nanotubes*, Phys. Stat. Sol. (b) **243**, 3403 (2006).

25. S. Berber, Y.-K. Kwon, and D. Tománek, *Unusually High Thermal Conductivity of Carbon Nanotubes*, Phys. Rev. Lett. **84**, 4613 (2000).

26. W. Zhang, Z. Zhu, F. Wang, T. Wang, L. Sun, and Z. Wang, *Chirality dependence of the thermal conductivity of carbon nanotubes*, Nanotechnology **15**, 936 (2004).

27. G. Zhang and B. Li, *Thermal conductivity of nanotubes revisited: Effects of chirality, isotope impurity, tube length, and temperature*, J. Chem. Phys. **123**, 114714 (2005).

28. C. W. Chang, D. Okawa, A. Majumdar, and A. Zettl, *Solid-State Thermal Rectifier*, Science **314**, 1121 (2006).

29. P. Kim and C. M. Lieber, *Nanotube Nanotweezers*, Science **286**, 2148 (1999).

30. B. Gao, C. Bower, J. D. Lorentzen, L. Fleming, A. Kleinhammes, X. P. Tang, L. McNeil, Y. Wu, and O. Zhou, *Enhanced saturation lithium composition in ball-milled single-walled carbon nanotubes*, Chem. Phys. Lett. **327**, 69 (2000).

31. J. Kong, N. R. Franklin, C. Zhou, M. G. Chapline, S. Peng, K. Cho, and H. Dai, *Nanotube Molecular Wires as Chemical Sensors*, Science **287**, 622 (2000).

32. Q. H. Wang, M. Yan, and R. P. H. Chang, *Flat panel display prototype using gated carbon nanotube field emitters*, Appl. Phys. Lett. **78**, 1294 (2001).

33. S. J. Tans, A. R. M. Verscheueren, and C. Dekker, *Room temperature transistor based on a single carbon nanotube*, Nature **393**, 49 (1998).

34. R. Martel, V. Derycke, C. Lavoie, J. Appenzeller, K. K. Chan, J. Tersoff, and P. Avouris, *Ambipolar Electrical Transport in Semiconducting Single-Wall Carbon Nanotubes*, Phys. Rev. Lett. **87**, 256805 (2001).

35. M. Radosavljevic, J. Appenzeller, P. Avouris, and Knoch, *High performance of potassium n-doped carbon nanotube field-effect transistors*, Appl. Phys. Letters **84**, 3693 (2004).

36. N. Neophytou, D. Kienle, E. Polizzi, and M. P. Anantram, *Influence of defects on nanotube transistor performance*, Appl. Phys. Lett. **88**, 242106 (2006).

37. L. Sun, F. Banhart, A. V. Krasheninnikov, J. A. Rodríguez-Manzo, M. Terrones, and P. M. Ajayan, *Carbon Nanotubes as High-Pressure Cylinders and Nanoextruders*, Science **312**, 1199 (2006).

38. P. Hohenberg and W. Kohn, *Inhomogenous Electron Gas*, Phys. Rev. **136**, B864 (1964).

39. W. Kohn and L. J. Sham, *Self-Consistent Equations Including Exchange and Correlation Effects*, Phys. Rev. **140**, A1133 (1965).

40. J. M. Thijssen, *Computational Physics* (Cambridge University Press, United Kingdom, 1999).

41. G. Kresse and J. Furthmüller, *Efficient iterative schemes for ab initio total-energy calculations using a plane-wave basis set*, Phys. Rev. B **54**, 11169 (1996).

42. P. E. Blöchl, *Projector augmented-wave method*, Phys. Rev. B **50**, 17953 (1994).

43. G. Kresse and J. Joubert, *From ultrasoft pseudopotentials to the projector augmented-wave method*, Phys. Rev. B **59**, 1758 (1999).

44. J. P. Perdew, J. A. Chevary, S. H. Vosko, K. A. Jackson, M. R. Pederson, D. J. Singh, and C. Fiolhais, *Atoms, molecules, solids, and surfaces: Applications of the generalized gradient approximation for exchange and correlation*, Phys. Rev. B **46**, 6671 (1992).

45. J. C. Slater and G. F. Koster, *Simplified LCAO Method for the Periodic Potential Problem*, Phys. Rev. **94**, 1498 (1954).

46. T. Frauenheim, G. Seifert, M. Elstner, T. Nichaus, C. Köhler, M. Amkreutz, M. Sternberg, Z. Hajnal, A. Di Carlo, and S. Suhai, *Atomistic simulations of complex materials: ground-state and excited-state properties*, J. Phys.: Condens. Matter **14**, 3015 (2002).

47. W. M. C. Foulkes and R. Heydock, *Tight-binding models and density-functional theory*, Phys. Rev. B **39**, 12520 (1989).

48. M. P. Allen and D. J. Tildesley, *Computer simulation of liquids* (Oxford University Press Inc., USA, 1987).

49. B. T. Alder and T. E. Wainright, *Studies in molecular dynamics. I. General method*, J. Chem. Phys. **31**, 459 (1959).

50. B. T. Alder and T. E. Wainright, *Studies in Molecular Dynamics. II. Behaviour of a small number of elastic spheres*, J. Chem. Phys. **33**, 1439 (1960).

51. R. Car and M. Parrinello, *Unified Approach for Molecular Dynamics and Density-Functional Theory*, Phys. Rev. Lett. **55**, 2471 (1985).

52. K. Nordlund, *Molecular dynamics simulation of ion ranges in the 1 - 100 keV energy range*, Comp. Mat. Sci. **3**, 448 (1995).

53. S. M. Foiles, *Application of the embedded-atom method to liquid transition metals*, Phys. Rev. B **15**, 3409 (1985).

54. S. M. Foiles, M. I. Baskes, and M. S. Daw, *Embedded-atom-method functions for the fcc metals Cu, Ag, Au, Ni, Pd, Pt, and their alloys*, Phys. Rev. B **33**, 7983 (1986).

55. J. Tersoff, *New empirical model for the structural properties of silicon*, Phys. Rev. Lett. **56**, 632 (1986).

56. K. Nordlund, J. Keinonen, and T. Mattila, *Formation of ion irradiation-induced small-scale defects on graphite surfaces*, Phys. Rev. Lett. **77**, 699 (1996).

57. H. J. C. Berendsen, J. P. M. Postma, W. F. van Gunsteren, A. DiNola, and J. R. Haak, *Molecular dynamics with coupling to external bath*, J. Chem. Phys. **81**, 3684 (1984).

58. D. W. Brenner, O. A. Shenderova, J. A. Harrison, S. J. Stuart, B. Ni, and S. B. Sinnott, *A second-generation reactive empirical bond order (REBO) potential energy expression for hydrocarbons*, J.Phys.: Condens. Matter **14**, 783 (2002).

59. K. Matsunaga, C. Fisher, and H. Matsubara, *Tersoff potential parametrization for simulating cubic boron carbonitrides*, Jpn. J. Appl. Phys. **39**, L48 (2000).

60. P. Erhart and K. Albe, *Analytical potential for atomistic simulations of silicon, carbon and silicon carbide*, Phys. Rev. B **71**, 035211 (2005).

61. R. A. Johnson and D. J. Oh, *Analytic embebbed atom method for bcc metals*, J. Mater. Res. **4**, 1195 (1989).

62. A. B. Bortz, M. H. Kalos, and J. L. Lebowitz, *A New Algorithm for Monte Carlo Simulation of Ising Spin Systems*, J. Comput. Phys. **17**, 10 (1975).

63. W. M. Young and E. W. Elcock, *Monte Carlo studies of vacancy migration in binary ordered alloys: I*, Proc. Phys. Soc. **89**, 735 (1966).

64. K. A. Fichthorn and W. H. Weinberg, *Theoretical foundations of dynamical Monte Carlo Simulations*, J. Chem. Phys. **95**, 1090 (1991).

65. D. P. Landau and K. Binder, *A Guide to Monte Carlo Simulations in Statistical Physics* (Cambridge University Press, United Kingdom, 2000).

66. J. Kotakoski *et al.*, unpublished.

67. N. A. Marks, N. C. Cooper, D. R. McKenzie, D. G. McCulloch, P. Bath, and S. P. Russo, *Comparison of density-functional, tight-binding, and empirical methods for the simulation of amorpohous carbon*, Phys. Rev. B **65**, 075411 (2006).

68. J. W. Mayer and S. S. Lau, *Electronic Materials Science For Integrated Circuits in Si and GaAs* (MacMillan, New York, 1990).

69. F. Banhart, *Formation and transformation of carbon nanoparticles under electron irradiation*, Phil. Trans. R. Soc. Lond. A **362**, 2205 (2004).

70. H. Schittenhelm, D. B. Geohegan, G. E. Jellison, A. A. Puretzky, M. J. Lance, and P. F. Britt, *Synthesis and characterization of single-wall carbon nanotube-amorphous diamond thin-film composites*, Appl. Phys. Lett. **81**, 2097 (2002).

71. B. Q. Wei, J. D'Arcy-Gall, P. M. Ajayan, and G. Ramanath, *Tailoring structure and electrical properties of carbon nanotubes using kilo-electron-volt ions*, Appl. Phys. Lett. **83**, 3581 (2003).

72. D.-H. Kim, H.-S. Jang, C.-D. Kim, D.-S. Cho, H.-D. Kang, and H.-R. Lee, *Enhancement of the field emission of carbon nanotubes straightened by application of argon ion irradiation*, Chem. Phys. Lett. **378**, 232 (2003).

73. Y. J. Jung, Y. Homma, R. Vajtai, Y. Kobayashi, T. Ogino, and P. M. Ajayan, *Straightening Suspended Single Walled Carbon Nanotubes by Ion Irradiation*, Nano Lett. **4**, 1109 (2004).

74. M. S. Raghuveer, P. G. Ganesan, J. D'Arcy-Gall, G. Ramanath, M. Marshall, and I. Petrov, *Nanomachining carbon nanotubes with ion beams*, Appl. Phys. Lett. **84**, 4484 (2004).

75. H. M. Kim, H. S. Kim, S. K. Park, J. Joo, T. J. Lee, and C. J. Lee, *Morphological change of multiwalled carbon nanotubes through high-energy (MeV) ion irradiation*, J. Appl. Phys. **97**, 026103 (2005).

76. G. H. Jeong, R. Hatakeyama, T. Hirata, K. Tohji, K. Motomiya, T. Yaguchi, and Y. Kawazoe, *Formation and structural observation of cesium encapsulated single-walled carbon nanotubes*, Chem. Comm. **1**, 152 (2003).

77. F. Banhart, *Irradiation effects in carbon nanostructures*, Rep. Prog. Phys. **62**, 1181 (1999).

78. A. H. Nevidomskyy, G. Csányi, and M. C. Payne, *Chemically Active Substitutional Nitrogen Impurity in Carbon Nanotubes*, Phys. Rev. Lett. **91**, 105502 (2003).

79. Y. Ma, A. S. Foster, A. V. Krasheninnikov, and R. M. Nieminen, *Nitrogen in graphite and carbon nanotubes: Magnetism and mobility*, Phys. Rev. B. **72**, 205416 (2005).

80. R. S. Lee, H. J. Kim, J. E. Fisher, A. Thess, and R. E. Smalley, *Conductivity enhancement in single-walled carbon nanotube bundles doped with K and Br*, Nature **388**, 255 (1997).

81. A.M.Rao, P. C. Eklund, S. Bandow, A. Thess, and R. E. Smalley, *Evidence for charge transfer in doped carbon nanotube bundles from Raman scattering*, Nature **388**, 257 (1997).

82. T. Miyake and S. Saito, *Electronic structure of potassium-doped carbon nanotubes*, Physica B **323**, 219 (2002).

83. A. F. Hebard, M. J. Rosseinsky, R. C. Haddon, D. W. Murphy, S. H. Glarum, T. T. M. Palstra, A. P. Ramirez, and A. R. Kortan, *Superconductivity at 18 K in potassium-doped C_{60}*, Nature **350**, 600 (1991).

84. P. Chen, X. Wu, J. Lin, and K. L. Tan, *High H_2 uptake by alkali-doped carbon nanotubes under ambient pressure and moderate temperatures*, Science **285**, 91 (1999).

85. R. Droppa, Jr., C. T. M. Ribeiro, A. R. Zanatta, M. C. dos Santos, and F. Alvarez, *Comprehensive spectroscopic study of nitrogenated carbon nanotubes*, Phys. Rev. B **69**, 045405 (2004).

86. D. Srivastava, M. Menon, C. Daraio, S. Jin, B. Sadanadan, and A. M. Rao, *Vacancy-mediated mechanism of nitrogen substitution in carbon nanotubes*, Phys. Rev. B **69**, 153414 (2004).

87. M. Glerup, J. Steinmetz, D. Samaille, O. Stéphan, S. Enouz, A. Loiseau, S. Roth, and P. Bernier, *Synthesis of N-doped SWNT using the arc-discharge procedure*, Chem. Phys. Lett. **387**, 193 (2004).

88. X. Liu, T. Pichler, M. Knupfer, and J. Fink, *Electronic and optical properties of alkali-metal-intercalated single-walled carbon nanotubes*, Phys. Rev. B **67**, 125403 (2003).

89. H. Murakami, M. Sano, and K. Ichimura, *Hydrogen in potassium-doped carbon nanotubes studied by positron annihilation*, Rad. Phys. Chem. **68**, 545 (2003).

90. L. Grigorian, G. U. Sumanasekera, A. L. Loper, S. Fang, J. L. Allen, and P. C. Eklund, *Transport properties of alkali-metal-dopen single-wall carbon nanotubes*, Phys. Rev. B **58**, R4195 (1998).

91. A. Claye, S. Rahman, J. E. Fischer, A. Sirenko, G. U. Sumanasekera, and P. C. Eklund, *In situ Raman scattering studies of alkali-doped single wall carbon nanotubes*, Chem. Phys. Lett. **333**, 16 (2001).

92. R. T. Yang, *Hydrogen storage by alkali-doped carbon nanotubes - revisited*, Carbon **38**, 623 (1999).

93. C. Morant, J. Andrey, P. Prieto, D. Mendiola, J. M. Sanz, and E. Elizalde, *XPS characterization of nitrogen-doped carbon nanotubes*, Phys. Stat. Sol. **203**, 1069 (2006).

94. H. T. Soh, C. F. Quate, A. F. Morpurgo, C. M. Marcus, J. Kong, and H. Dai, *Integrated nanotube circuits: Controlled growth and ohmic contacting of single-walled carbon nanotubes*, Appl. Phys. Lett. **75**, 627 (1999).

95. A. Bachtold, M. Henny, C. Terrier, C. Strunk, C. Schonenberger, J.-P. Salvetat, J.-M. Bonard, and L. Forró, *Contacting carbon nanotubes selectively with low-ohmic contacts for four-probe electric measurements*, Appl. Phys. Lett. **73**, 274 (1998).

96. N. Nemec, D. Tománek, and G. Cuniberti, *Contact Dependence of Carrier Injection in Carbon Nanotubes: An* ab initio *study*, Phys. Rev. Lett. **96**, 076802 (2006).

97. L. Lechner, J. Kotakoski, O. Lehtinen, P. Hakonen, and J. Keinonen, unpublished.

98. A. V. Krasheninnikov, K. Nordlund, M. Sirviö, E. Salonen, and J. Keinonen, *Formation of ion irradiation-induced atomic-scale defects on walls of carbon nanotubes*, Phys. Rev. B **63**, 245405 (2001).

99. A. V. Krasheninnikov, K. Nordlund, and J. Keinonen, *Production of defects in supported carbon nanotubes under ion irradiation*, Phys. Rev. B **65**, 165423 (2002).

100. A. J. Stone and D. J. Wales, *Theoretical studies of icosahedral C_{60} and some related species*, Chem. Phys. Lett. **128**, 501 (1986).

101. C. P. Ewels, M. I. Heggie, and P. R. Briddon, *Adatoms and nanoengineering of carbon*, Chem. Phys. Lett. **351**, 178 (2002).

102. A. V. Krasheninnikov, K. Nordlund, L. P. O., A. S. Foster, A. Ayuela, and R. M. Nieminen, *Adsorption and migration of carbon adatoms on carbon nanotubes: Density-functional* ab initio *and tight-binding studies*, Phys. Rev. B **69**, 073402 (2004).

103. A. V. Krasheninnikov, P. O. Lehtinen, A. S. Foster, and R. M. Nieminen, *Bending the rules: Contrasting vacancy energetics and migration in graphite and carbon nanotubes*, Chem. Phys. Lett. **418**, 132 (2006).

104. C. P. Ewels, R. H. Telling, , A. A. El-Barbary, and M. I. Heggie, *Metastable Frenkel Pair Defect in Graphite: Source of Wigner Energy?*, Phys. Rev. Lett. **91**, 025505 (2003).

105. M. Sternberg, L. A. Curtiss, D. M. Gruen, G. Kedziora, D. A. Horner, P. C. Redfern, and P. Zapol, *Carbon Ad-Dimer Defects in Carbon Nanotubes*, Phys. Rev. Lett. **96**, 075506 (2006).

106. F. Banhart, J. X. Li, and M. Terrones, *Cutting Single-Walled Carbon Nanotubes with an Electron Beam: Evidence for Atom Migration Inside Nanotubes*, Small **1**, 953 (2005).

107. F. Banhart, J. X. Li, and A. V. Krasheninnikov, *Carbon nanotubes under electron irradiation: Stability of the tubes and their action as pipes for atom transport*, Phys.Rev.B **71**, 241408(R) (2005).

108. O. Lehtinen *et al.*, unpublished.